UDP-glucosyltransferase HvUGT13248 confers type II resistance to Fusarium graminearum in barley

Short title: Function of UGT13248 in barley

Title: *HvUGT13248* Confers Type II Resistance to *Fusarium graminearum* in Barley

Authors: Gerit Bethke[1,$], Yadong Huang[1,$], Goetz Hensel[2,#], Shane Heinen[1], Chaochih Liu[1], Skylar R. Wyant[1,§], Xin Li[1,ŧ], Maureen B. Quin[3], Susan McCormick[4], Peter L. Morrell[1], Yanhong Dong[5], Jochen Kumlehn[2], Silvio Salvi[6], Franz Berthiller[7], Gary J. Muehlbauer[1]*

[1] University of Minnesota, Department of Agronomy and Plant Genetics, Saint Paul, MN, USA

[2] Leibniz Institute of Plant Genetics and Crop Plant Research (IPK), Plant Reproductive Biology, Gatersleben, Germany

[3] University of Minnesota, Biotechnology Institute, Saint Paul, MN, USA

[4] USDA-ARS NCAUR, Mycotoxin Prevention and Applied Microbiology Research, Peoria IL, USA

[5] University of Minnesota, Department of Plant Pathology, Saint Paul, MN, USA

[6] University of Bologna, Department of Agricultural and Food Sciences, Bologna, Italy

[7] University of Natural Resources and Life Sciences, Vienna (BOKU), Department of Agrobiotechnology, Tulln, Austria

[$] These authors contributed equally to this work.

[#] Current affiliation: Heinrich-Heine-University, Centre for Plant Genome Engineering (CPGE), Düsseldorf, Germany

[ŧ] Current affiliation: Department of Plant and Microbial Biology, North Carolina State University, Raleigh, NC 27695; and Plants for Human Health Institute, North Carolina State University, Kannapolis, NC 28081, USA

[§] Current affiliation: Dept. of Ecology and Evolutionary Biology, University of California, Irvine, Irvine, CA 92697- 2525, USA

Abstract

Fusarium head blight (FHB) of barley (*Hordeum vulgare*) causes yield losses and accumulation of trichothecene mycotoxins (e.g. deoxynivalenol (DON)) in grains. Glucosylation of DON to the nontoxic DON-3-*O*-glucoside (D3G) is catalyzed by UDP-glucosyltransferases (UGTs), e.g. barley UGT13248. We explored the natural diversity of *UGT13248* in 496 barley accessions and showed that all accessions tested likely carried functional alleles of *UGT13248*, as no genotypes tested showed strongly increased seedling sensitivity to DON. From a TILLING population, we identified two mutant alleles (T368I and H369Y) that, based on protein modeling, likely affect UDP-glucose binding of UGT13248. In DON feeding experiments, DON to D3G conversion was strongly reduced in spikes of these mutants compared to controls and plants overexpressing UGT13248 showed increased resistance to DON and increased DON to D3G conversion. Moreover, field grown plants carrying the T368I and H369Y mutations inoculated with *F. graminearum* showed increased FHB disease severity and reduced D3G production. Barley is generally considered to have type II resistance that limits the spread of *F. graminearum* from the infected spikelet to adjacent spikelets. Point inoculation experiments with *F. graminearum* showed increased spread of infection in T368I and H369Y across the spike compared to wild-type, while overexpression plants showed decreased spread of FHB symptoms. Confocal microscopy revealed that *F. graminearum* spread to distant rachis nodes in T368I and H369Y, but was arrested at the rachis node of the inoculated spikelet in wild-type plants. Taken together, UGT13248 confers type II resistance to FHB in barley via conjugation of DON to D3G.

INTRODUCTION

Fusarium Head Blight (FHB) is a devastating disease of small-grain cereals and can lead to severe crop losses by reducing crop yield and grain quality (Bai et al., 2018; Chen et al., 2019; Johns et al., 2022). It is caused by several species of the fungal genus *Fusarium. Fusarium graminearum* (teleomorph *Gibberella zeae*) is considered to be the primary cause of FHB in cereal crops globally, especially in wheat (Starkey et al., 2007; Xu and Nicholson, 2009). *Fusarium spp.* produce several groups of mycotoxins, including trichothecenes, zearalenone, beauvericin, enniatins and fumonisins (Ferrigo et al., 2016; McCormick et al., 2011; Santini et al., 2012). Trichothecenes are a large family of sesquiterpenoids defined by their heterocyclic structure, which includes a 9,10-double bond and a 12,13-epoxide (Chen et al., 2019). Type B trichothecene mycotoxins, characterized by a keto group at C-8, are produced during *Fusarium*-plant interactions and include deoxynivalenol (DON), nivalenol (NIV), 15-*O*-acetyl-DON, and 3-*O*-acetyl-DON (McCormick et al., 2011; Varga et al., 2015), of which DON and NIV are among the most frequently detected mycotoxins in cereal grains worldwide (Lee and Ryu, 2017). The more recently discovered NX-toxins, such as the prominent NX-3 are structural analogs, but lack the C-8 keto-group (Varga et al., 2015). Trichothecene mycotoxins inhibit protein biosynthesis (McLaughlin et al., 1977) and their accumulation is coincident with the switch between biotrophic and necrotrophic growth of *F. graminearum*, indicating they play an important role in infection (Bushnell et al., 2003).

The biosynthetic enzymes for trichothecene production are encoded by 15 *TRI* genes in *F. graminearum* (Chen et al., 2019). The *TRI5* gene encodes trichodiene synthase, which is the first enzyme in the trichothecene biosynthetic pathway, and cyclizes farnesyl pyrophosphate to trichodiene (Hohn and Beremand, 1989). The ability of *F. graminearum* to produce trichothecenes is a prerequisite for full pathogenicity and fungal spread in wheat spikes, as *tri5* mutants can initially infect wheat, but the infection is restricted to the rachis node of the infected spikelet and does not spread throughout the spike (Bai et al., 2001; Jansen et al., 2005; Proctor et al., 1995). Hence, in wheat, tolerance to trichothecenes is required for the ability to limit spread of the infection in the spike (type II resistance), but not resistance to initial infection (type I resistance) (Jansen et al., 2005; Schroeder and Christensen, 1963). Conversion

of DON to DON-3-*O*-glucoside (D3G) reduced toxicity on wheat ribosomes (Poppenberger et al., 2003) and co-segregated with a major FHB resistance QTL (*Fhb1*) in wheat (Lemmens et al., 2005). UDP-glucosyl transferases (UGTs) catalyze DON to D3G conversion by transferring glucose from the UDP-glucose substrate to the hydroxyl group of carbon 3 of DON (Poppenberger et al., 2003). Heterologous expression of the barley *UGT13248* gene in wheat resulted in increased type II resistance to *F. graminearum,* underscoring the role of DON in overcoming type II resistance to FHB in wheat (Li et al., 2015).

In contrast to wheat, barley is generally considered to have innate type II resistance, and extensive spread of the disease throughout the spike is rare (Boddu et al., 2007; Steffenson, 2003). Thus, FHB impacts the yield of wheat more than barley. However, because the lemma and palea are retained on barley kernels throughout harvest and processing, barley can accumulate high levels of mycotoxins, which are problematic for human and animal health (Steffenson, 2003). No major FHB resistance locus affecting plant immune signaling or biochemistry has been identified in barley to date. FHB resistance in barley is quantitatively inherited, and QTL associated with resistance are also associated with multiple agro-morphological traits that influence resistance, including plant height, heading date, spike morphology, including row type and spike density, as well as grain protein content (de la Peña et al., 1999; Huang et al., 2021; Massman et al., 2011; Mesfin et al., 2003; Zhu et al., 1999). Interestingly, while wild-type *F. graminearum* grew through the rachis node in the wheat cv. 'Nandu' and a *tri5* mutant strain was restricted at the rachis node, both of these strains were arrested at the rachis node in the barley cv. 'Chevron' (Jansen et al., 2005). This demonstrates a strong correlation between trichothecene production and FHB disease progression in wheat, while the relationship between FHB disease progression and trichothecene production in barley remains unclear.

UDP-glucosyl transferases (UGTs) have been studied and functionally characterized in multiple plant species, and some of them have been shown to detoxify DON. In *Arabidopsis thaliana,* a cluster of six UGTs was identified, of which UGT73C5 (DOGT1) and UGT73C4, were found to convert DON to D3G (Poppenberger et al., 2003; Schweiger et al., 2010). In barley, nine UGT genes were upregulated in response to *F. graminearum* (Boddu et al., 2006), three

UGT genes were expressed in response to a wild-type *F. graminearum* but not a *tri5* mutant strain (Boddu et al., 2007) and two UGTs were expressed in DON- but not water-treated barley plants (Gardiner et al., 2010). Four of these barley UGTs, UGT14077, UGT5876, UGT13248 and UGT19290, were expressed in yeast and grown on DON-containing media and only UGT13248 was found to convert DON to D3G (Schweiger et al., 2010). Interestingly, the closest homolog to DOGT1 in barley, UGT5876, did not show activity to DON in yeast (Schweiger et al., 2010), suggesting that close protein homology does not necessarily predict substrate specificity in these proteins. Further, UGT14077 was found to glucosylate another *Fusarium* toxin, zearalenone (Michlmayr et al., 2017). Heterologous expression of UGT13248 in *Arabidopsis thaliana* and wheat resulted in DON-resistant seedlings and reduced FHB severity, respectively (Li et al., 2015; Shin et al., 2012). Both transgenic *Arabidopsis* and wheat rapidly conjugated DON to D3G. UGTs that glucosylated DON were identified in wheat (He et al., 2020; Kirana et al., 2022), *Aegilops tauschii* (Kirana et al., 2022), rice (Schweiger et al., 2013), sorghum (Schweiger et al., 2013) and *Brachypodium distachyon* (Schweiger et al., 2013). In *B. distachyon,* two UGTs Bradi5g03300, the closest *Brachypodium* homolog to barley UGT13248, and Bradi5g02780 were shown to catalyze DON to D3G conversion in yeast (Schweiger et al., 2013). Plants with mutations in Bradi5g03300 showed similar colonization upon point inoculation with *F. graminearum* as compared to wild-type *Brachypodium* plants. Moreover, they were more susceptible when spray inoculation was used, suggesting that Bradi5g03300 is involved in type I, but not type II resistance in *Brachypodium* (Pasquet et al., 2016). Bradi5g03300 overexpression plants also showed increased root tolerance to DON (Pasquet et al., 2016).

Crystal structures for *Os*79, a rice UGT with high homology to UGT13248, complexed with the nonreactive co-substrate analog UDP-2-deoxy-2-fluoroglucose and trichothecene, which lacks the C3 hydroxyl group to which the glucose molecule is attached, as well as with UDP alone were reported (Wetterhorn et al., 2016). The *Os*79 structure is similar to other known plant UGTs and contain the plant secondary product glycosyltransferase (PSPG) motif, a hallmark of UGT enzymes, which is considered part of the region interacting with the UDP-sugar co-substrate (Gachon et al., 2005; Vogt and Jones, 2000; Wetterhorn et al., 2016). The active site of *Os*79 is located in a cleft between the *C*-terminal donor-binding and the *N*-terminal

acceptor domains (Wetterhorn et al., 2016). Using structural alignments, it was shown that *Os*79 likely utilizes a catalytic mechanism similar to those of other plant UGTs, where His 27 activates the trichothecene O3 hydroxyl for nucleophilic attack at C1 of the UDP-glucose donor molecule (Wetterhorn et al., 2016). Kinetic analysis of *Os*79 mutants identified Thr 291 as required to position the UDP moiety during the nucleophilic attack or for catalysis as a catalytic acid (Wetterhorn et al., 2016). *Os*79 conjugates multiple trichothecene substrates such as DON, nivalenol, isotrichodermol, and HT-2 toxin, but not T-2 toxin (Wetterhorn et al., 2016). Interestingly, three mutations in *Os*79 yielded a H122A/L123A/Q202L Os79 triple mutant that had an increased active site volume and showed activity on T-2 toxin (Wetterhorn et al., 2017). UGT13248 was able to conjugate nivalenol, whereas DOGT1 was not (Li et al., 2017).

DON is a virulence factor in wheat and detoxification of DON is clearly linked to increased type II resistance. However, it is unclear if this is true in other grasses, including *B. distachyon* and barley. We decided to study UGT13248 directly in barley to understand if detoxification of DON by conversion to D3G affects FHB disease progression in this crop. We first investigated natural variation in *UGT13248* to identify UGT13248 variants with altered function. In 496 barley accessions tested, no UGT13248 alleles that abolished function were identified, suggesting that UGT13248 function is highly conserved throughout the species. We next identified mutations with reduced UGT13248 function and plants overexpressing *UGT13248* to study the role of UGT13248 in barley-*Fusarium* interactions in detail. We found that UGT13248 confers type II resistance to *F. graminearum* in barley.

RESULTS

Many barley accessions contain functional UGT13248 alleles

Our previous research showed that barley UGT13248 converts DON to D3G in wheat, *Arabidopsis* and yeast (Li et al., 2015; Schweiger et al., 2010; Shin et al., 2012). Overexpression of UGT13248 in wheat resulted in rapid DON to D3G conversion and reduced FHB prevalence (Li et al., 2015). Here, we aimed to understand the function of UGT13248 directly in barley. Multiple groups have identified QTLs in barley that affect DON accumulation and FHB severity

(Huang et al., 2018; Massman et al., 2011); however, ~~the QTLs found generally affected agro-morphological traits including plant height, heading date, or spike morphology (Massman et al., 2011; Mesfin et al., 2003; Zhu et al., 1999).~~ *UGT13248* has not been identified as a contributor to FHB resistance in any of these QTL studies (Huang et al., 2018; Massman et al., 2011). We decided to screen a natural population of barley accessions for mutations in *UGT13248* that might affect UGT13248 function. First, we compared the UGT13248 protein sequences of eight susceptible and 18 resistant barley accessions (Supplemental Table 1; (Huang et al., 2013). We considered the *UGT13248* sequence of cv. 'Morex', used for the first barley whole genome sequencing project (Mayer et al., 2012), the wild-type allele, as UGT13248 was identified initially in this cultivar (GU170355; (Schweiger et al., 2010). In these 26 accessions, two non-synonymous mutations were found. A104V was found in seven accessions and G213R in two accessions (Supplemental Figure 1A and Supplemental Table 1). Of these, only G213R was exclusively found in two accessions that are susceptible to FHB, PI383933, and ICB111809 (Huang et al., 2013). We grew representative accessions that carried *UGT13248* alleles representing each mutation, and wild-type Morex plants on mock and DON-containing media and measured seedling root length for six days. While seedling root length on DON-containing media was reduced in the cv. 'Fredrickson' that carried the A104V mutations, other accessions carrying the same mutation did not show significantly reduced root growth (Supplemental Figure 1 B-D). None of the accessions containing mutations in *UGT13248* showed severely reduced root growth on DON-containing media (Supplemental Figure 1 B-D), suggesting that none of the mutations had a drastic effect on DON-induced root growth inhibition.

We next analyzed the *UGT13248* sequences of 19 additional barley accessions, sequenced as part of a barley pan-genome analysis (Jayakodi et al., 2020). We identified A104V in six additional accessions and G213R in seven additional accessions (Supplemental Figure 1A and Supplemental Table 1). We also identified an additional mutation in the accession FT 11/ B1K-04-12, corresponding to R47H (Supplemental Figure 1A). No difference in seedling root growth was observed between mock and DON-containing media for FT11 (Supplemental Figure 1E).

We next utilized protein modeling as a predictive tool to develop hypotheses if these mutations potentially affect UGT13248 function. SWISS MODEL blast identified the closest homolog to UGT13248 at 73 % amino acid sequence identity as rice *Os*79, for which a crystal structure has been resolved (Wetterhorn et al., 2016). We aligned the sequence used for the *Os*79 crystal structure (PDB ID: 5TMD), the full-length *Os*79 protein sequence, and the UGT13248 protein sequence (Supplemental Figure 2A). We used the *Os*79 three-dimensional structure with trichothecene and the nonreactive co-substrate analog UDP-2-deoxy-2-fluoroglucose modeled within the active site cavity as a template for barley UGT13248 protein models. The resulting homology models of UGT13248 exhibited a similar Rossman-fold type three-dimensional structure as *Os*79. In *Os*79, the proposed catalytic residues for initiating the glycosylation of trichothecene via deprotonation of the hydroxyl group are H27 and D120, while T291 is hypothesized to be involved in coordinating the UDP during the subsequent nucleophilic attack. Based on sequence alignments, the corresponding UGT13248 residues that could be hypothesized to act as the catalytic dyad are H38 and D130, and T299 could serve as the UDP-coordinating group (Supplemental Figure 2A). The homology models indicated that these three residues would likely be structurally positioned within an active site pocket similar to that of *Os*79 and, therefore may be important for the correct function of UGT13248 (Supplemental Figure 2B). The structural positions of mutated residues in models of R47H, A104V, and G213R, indicated that these amino acids are not within close proximity with the UDP-glucose and trichothecene molecules (Supplemental Figure 2C-E). It was therefore considered less likely that these mutations would influence UGT13248 function.

To explore the genetic diversity of *UGT13248* in a larger natural population, we utilized previously-generated exome capture sequencing data (Chen et al., 2022; Hemshrot et al., 2019; Kono et al., 2019; Lei et al., 2019; Mascher et al., 2013; Nice et al., 2016; Russell et al., 2016) to screen for mutations in *UGT13248*. The data set included 83 elite lines, 188 wild barley accessions and 187 landraces. The exome capture sequencing data covered two regions of the Morex UGT13248 gene. One region covered a portion of exon 1 and intron 1, and the other region covered the majority of exon 2, intron 2, and exon 3 (Supplemental Figure 3A). The second region contains the PSPG box (Gachon et al., 2005; Vogt and Jones, 2000), thought to be

important for UDP-glucose binding, as well as the predicted residue for UDP positioning T299 that had been identified during homology modeling (Supplemental Figure 2A). From this analysis, nine non-synonymous mutations were identified in 64 of these 458 accessions. These nine non-synonymous mutations were G213R, M281I, D282N, F385S, S403I, L419V, Y440L, S461P and F468L (Supplemental Figure 3A). G213R, which we identified in nine of the 45 barley accessions with full-length genomic DNA sequence data (Supplemental Table 1), was found in an additional 38 landraces and 3 elite cultivars using the exome capture sequencing approach (Supplemental Table 2). The other eight non-synonymous mutations were identified in seven landraces and 16 wild barley accessions (Supplemental Table 2). Analysis of the protein homology models of these mutants indicated that the mutated residues M281I, D282N, F385S, S403I, L419V, Y440L, S461P, and F468L were not structurally positioned within the catalytic site, leading us to hypothesize that none of these mutations would directly influence UGT13248 catalytic function (Supplemental Figure 3B-I). To confirm, we screened 14 accessions, representing these other eight non-synonymous *UGT13248* mutations, and measured seedling root growth on mock and DON-containing media. Seedling root length on DON-containing media was slightly, but significantly reduced in FT222, which carries the M281I mutation, FT735 that carries the F468L mutation, as well as two of six accessions that carry the D282N mutation, Hor2867, and PI57099 (Supplemental Figure 4 A, B, D and E). None of the accessions tested however exhibited a complete inhibition of root growth upon DON exposure (Supplemental Figure 4), suggesting that the mutations M281I, D282N, F385S, S403I, L419V, Y440L, S461P, and F468L did not have a deleterious effect on UGT13248-dependent DON to D3G conversion. Overall, none of the 11 mutations, identified in the 496 accessions analyzed, had a strong adverse effect on UGT13248 activity and all these lines likely contained functional UGT13248 alleles. ~~Taken together, we conclude that mutations in UGT13248 are rare and likely do not disrupt UGT 13248 protein function.~~

Mutations in UGT13248 or constitutive expression of UGT13248 affect root sensitivity to DON

To further study the role of UGT13248 in barley, we decided to utilize plants that constitutively express UGT13248. We transformed *UGT13248* under the control of the constitutive *Zea mays*

Ubiquitin (*Ubi-1*) promotor into the barley cultivar 'Golden Promise' (Supplemental Figure 5A). We identified three independent insertion lines in Golden Promise (Supplemental Figure 5B). As Golden Promise does not reliably flower under our growth conditions, we crossed the transgenic lines with the cultivar 'Rasmusson'. We backcrossed the plants once with Rasmusson and then identified sets of sister lines that contained and expressed the *UGT13248* ~~transgene~~ transcript and the UGT13248 protein (UGT+) or did not contain either (UGT-) from two independent transgenic events (#39003 and #39009) (Supplemental Figure 5C and E). For both sets of sister lines the accession containing the transgene and expressing UGT13248 (UGT+) did not show significantly reduced seedling root growth two to six days after DON treatment, while the non-transgenic UGT- lines, as well as Golden Promise and Rasmusson wild-type seedlings did (Figure 1A and B). We conclude that overexpression of UGT13248 increases root resistance to DON application.

We also screened a TILLING population in the barley cultivar Morex (TILLMore; (Talame et al., 2008a) for UGT13248 mutations. We identified three lines that contained non-synonymous mutations T368I, H369Y, and S403N. Two of the three lines, T368I and H369Y, exhibited strongly reduced seedling root growth two to six days after transfer to DON-containing media when compared to wild-type Morex plants (Figure 1C and D). S403N plants were indistinguishable from Morex plants (Figure 1C). Additionally, we crossed the H369Y and T368I plants to Morex and analyzed the resulting F_2 population. Upon exposure to DON the roots of homozygous T368I and H369Y mutants were significantly shorter than roots of homozygous wild-type and heterozygous plants (Supplemental Figure 6A and B). We conclude that plants carrying the T368I and H369Y mutations of UGT13248, but not the S403N mutation, have reduced UGT13248 function.

Protein models suggest that UGT13248 T368I and H369Y variants might have altered substrate binding

To further understand the effect of the T368I and H369Y mutations on UGT13248 function, we created protein models for UGT13248 carrying the T368I, H369Y, and S403N mutations and

compared these to the wild-type UGT13248 protein model (Figure 2). According to the protein models that were generated, amino acids T368 and H369 are located within 4 Å of the UDP-glucose molecule. Thus, we hypothesized that these two residues may contribute to the hydrogen bonding network for the stabilization of UDP at the active site (Figure 2). In the *Os*79 crystal structure, residue T291 was proposed to be involved in either the positioning of the substrate, or in protonation (Wetterhorn et al., 2016). In the UGT13248 protein homology model, T368 is positioned within hydrogen bonding distance of H369, which in turn is positioned within hydrogen bonding distance of UDP-glucose. Therefore, T368 and H369 may be required for positioning of substrate within the active site. On the other hand, in the UGT13248 protein homology model, S403 is distant (>4 Å) from the active site and is therefore not expected to be involved in substrate binding. This may explain why the mutant S403N roots did not show increased susceptibility to DON.

Interestingly, we noted in the protein model that when the polar residue threonine is replaced by a hydrophobic isoleucine (T368I), the hydrogen bond between a hydroxyl side chain and the nitrogen atom of H369 is disrupted, which could potentially indicate an impact on the hydrogen bonding network surrounding the substrate. Furthermore, when the charged residue histidine is replaced by hydrophobic tyrosine (H369Y) in the protein model, the negatively charged hydroxyl group of the tyrosine side chain has the potential to cause steric hindrance of UDP, possibly inhibiting correct substrate binding within the active site (Figure 2).

Taken together, these differences in the protein models suggest that the T368I and H369Y mutations could affect UGT134248 function by influencing the binding of the UDP-glucose substrate, potentially impacting the enzyme function, which may explain the increased sensitivity to DON demonstrated in plants carrying these mutations.

UGT13248 is required for DON to D3G conversion

To test the effect of UGT13248 overexpression on DON to D3G conversion, we inoculated spikes of #39003_UGT- and #39003_UGT+ sister lines with DON at anthesis. We measured DON and D3G levels 0 h, 4 h, 24 h, 48 h, and 96 h after inoculation. UGT- plants that do not contain

303 the transgene, showed some increase in D3G / DON over time, while the D3G / DON ratio was
304 significantly increased in UGT+ plants at 24 h, 48 h, and 96 h (Figure 3A). To better understand
305 the dynamics of *UGT13248* expression in these genotypes, we used qRT-PCR to compare
306 expression of the endogenous *UGT13248* and the *UGT13248-FLAG* transgene in mock- and
307 DON-treated UGT- and UGT+ plants (Supplemental Figure 5D). UGT+ and UGT- plants showed
308 similar levels of endogenous *UGT13248* in mock treated samples at 0 h, 4 h, and 24 h after
309 inoculation. In UGT- plants a strong increase in endogenous *UGT13248* was detected at 4 h and
310 24 h after DON inoculation. In UGT+ plants an increase of endogenous *UGT13248* expression
311 was detected at 4 h, but not 24 h after DON application. In addition to the endogenous
312 *UGT13248*, UGT+ plants expressed the *UGT13248-FLAG* transgene at a constitutive and
313 elevated level compared to endogenous *UGT13248*. The total amount of *UGT13248* expression
314 in UGT+ plants is higher compared to UGT- plants at 0 h, 4 h, and 24 h after mock treatment
315 and at 0 h and 4 h after DON application. The combined level of *UGT13248-FLAG* and
316 endogenous *UGT13248* expression in UGT+ plants is similar to the endogenous *UGT13248*
317 expression in UGT- plants at 24 h after DON treatment. This suggests that *UGT13248* expression
318 is upregulated upon DON application. It is possible that the level of *UGT13248* expression is
319 regulated by a feedback mechanism that prohibits continued *UGT13248* expression in response
320 to DON after a certain *UGT13248* expression level is reached or alternatively, DON to D3G
321 conjugation might reduce available DON concentrations and thus reduce DON-induced
322 *UGT13248* gene expression. Taken together, the data show that UGT13248 converts DON to
323 D3G in barley and that earlier and higher levels of *UGT13248* lead to increased conversion of
324 DON to D3G.

325 To understand the effect of altered UDP-glucose binding on UGT13248 function in more
326 detail, T368I, H369Y, S403N, and Morex spikes were inoculated with DON at anthesis. DON and
327 D3G were measured at 0 h, 12 h, 24 h, 48 h, and 96 h after inoculation. T368I and H369Y plants
328 showed significantly reduced D3G / DON accumulation at 24 h, 48 h, and 96 h, compared to
329 Morex and S403N plants (Figure 3B). This shows that the T368I and H369Y mutations inhibit
330 UGT13248-dependent DON to D3G conversion.

331

UGT13248 mutants have increased susceptibility to FHB in the field

We performed field evaluations to investigate the effect of the reduced UGT13248 activity on FHB severity and DON and D3G accumulation upon plant infection with *F. graminearum*. Field evaluations of Morex, T368I, H369Y, and S403N plants were performed in two years, 2019 and 2020, and in two different field locations in Minnesota, Saint Paul and Crookston. No differences in plant height were observed between Morex and any of the mutants in three environments (Supplemental Figure 7A-C). In Saint Paul, plants were spray-inoculated at anthesis and in Crookston grain spawn inoculation was used. In all four environments T368I plants showed significantly increased FHB severity compared to wild-type Morex, while S403N plants did not. In three out of four environments (Saint Paul, 2020, Crookston, 2019 and Crookston, 2020) H369Y plants showed significantly increased FHB severity compared to wild-type Morex (Figure 4A and B). FHB disease development is influenced by many factors including temperature and humidity thus it is not unusual to see variation of FHB severity in different environments (Steffenson, 2003). We conclude that H369Y and T368I plants, that have strongly reduced UGT13248 activity, are more susceptible to *F. graminearum*.

DON and D3G accumulation were measured in plants from the Saint Paul trial in 2019 and 2020 (Supplemental Figure 7D-G). In both years, the ratio of D3G to DON was significantly reduced in T368I and H369Y plants compared to wild-type Morex and S403N plants from 14 days after inoculation to harvest (30-32 days after inoculation) (Figure 4C and D). Thus, even in the environment that we did not detect any increased FHB severity for H369Y (Saint Paul 2019), we still detected a robust reduction in the conversion of DON to D3G in H369Y plants under field conditions.

Point inoculation experiments suggest a role of UGT13248 in type II resistance in barley

~~It has previously been shown that *F. graminearum* produces DON during the infection process (Evans et al., 2000) and that trichothecenes are virulence factors in wheat (Proctor et al., 1995).~~ To gain a more detailed understanding of the effect of UGT13248 on FHB disease progression in barley, we used point inoculation experiments on UGT13248 mutants and overexpression

plants. We inoculated the two central spikelets in the middle of each spike on either side of the spike with *F. graminearum* strain PH-1 and monitored FHB severity over time. In both sets of UGT13248 overexpression plants (#39003 and #39009), the UGT+ individuals, carrying the UGT13248 transgene, showed significantly increased resistance to *F. graminearum* at 7 and 11 days after inoculation compared to the UGT- sister lines (Figure 5B). The UGT+ (39009) plants also showed significantly decreased susceptibility at 14 and 21 days after infection compared to their UGT- (39009) sister line, while no significant difference could be detected between the second set of sister lines (39003) (Figure 5A and B). In the case of the 39003 sister lines, the UGT+ plants were shorter and showed increased spike density compared to the UGT- individuals (Supplemental Figure 8), which likely increased disease progression at the later time points in the UGT+ plants. We conclude that UGT13248 overexpression leads to increased type II resistance to *F. graminearum* at least early after infection with *F. graminearum*.

Next, point inoculation experiments were performed for Morex, T368I, H369Y, and S403N plants. While FHB symptoms were restricted to one to two rows of spikelets basipetal and acropetal each from the inoculated spikelets in Morex and S403N, symptoms spread much further in T368I and H369Y plants (Figure 5C). T368I and H369Y plants, which have strongly reduced UGT13248 activity showed significantly increased FHB severity at 7, 11, and 14 days after inoculation when compared to wild-type Morex and S403N plants (Figure 5D). We conclude that DON to D3G conversion by UGT13248 is a major contributor to type II resistance in barley.

Differences in susceptibility to *F. graminearum* in the field are not primarily dependent on differences in type II resistance

We utilized a set of barley genotypes to determine if point inoculation can reproduce differences in FHB severity previously described under field conditions. We inoculated the resistant cultivars Chevron, Quest, Stellar, and Frederickson and the susceptible accessions Morex, PI383933, ICB111809, and Stander, together with the H369Y plants. Only the highly susceptible accession PI383933 (Huang et al., 2013) and H369Y plants showed very high FHB

severity, while all other genotypes showed comparable FHB severity (Supplemental Figure 9A). We also plotted the average number of diseased spikelets in each genotype (Supplemental Figure 9B) as this may be a truer representation of fungal spread as different genotypes had different total numbers of spikelets or rachis nodes, and the tested genotypes were comprised of 2-row and 6-row accessions. The 2-row accessions Fredrickson and ICB111809 showed the lowest number of diseased spikelets, the 6-row accessions Chevron, Morex, Stander and Stellar showed slightly higher numbers of diseased spikelets, the 6-row accession PI383933 showed a higher number of diseased spikelets and the 6-row accession Quest showed an intermediate number of diseased spikelets compared to PI383933 and Chevron, Morex, Stander and Stellar. However, the number of diseased spikelets was significantly higher in H369Y plants compared to all other genotypes tested (Supplemental Figure 9B).

PI383933 plants are very short and have short, dense spikes ((Huang et al., 2018), Supplemental Figures 8 C-E). While PI383933 plants contain the G213R mutations of UGT13248, PI383933 seedlings did not show high sensitivity to DON (Supplemental Figure 1C), suggesting that they carry a functional UGT13248 allele. Additionally, in a mapping population of a cross between Rasmusson and PI383933 (Huang et al., 2018), taller plants were generally more resistant to FHB and shorter plants were generally more susceptible to FHB. This was independent of the Rasmusson or PI383933 *UGT13248* allele they carried, but dependent on plant height (Supplemental Figure 10 B). We also observed that the spikelets on the tip of the PI383933 spikes remained green in individuals with less than 100% FHB severity, while the terminal florets in H369Y plants were bleached (Supplemental Figure 10 A). Thus, susceptibility of PI383933 to *F. graminearum* is likely due to plant morphology rather than reduced type II resistance.

Taken together, this suggests that FHB susceptibility in the field is not likely predominantly dependent on differences in type II resistance, but rather type I resistance, row-type, and various agro-morphological traits that do not affect FHB development upon point inoculation under controlled growth conditions.

Fusarium graminearum spreads through the rachis of T368I and H369Y but is restricted to the inoculated rachis node in wild-type barley plants

Previously, Jansen *et al*. (Jansen et al., 2005) studied the spatiotemporal dynamics of *F. graminearum* infection in wheat and barley using a GFP-labeled wild-type *F. graminearum* strain as well as a strain lacking trichothecene production. The authors found that in barley both the wild-type and the trichothecene knockout strain were inhibited at the rachis node of the infected spikelet. We used the H369Y and Morex plants to study if UGT13248 was required for blocking *F. graminearum* invasion of the rachis. We inoculated ~~the~~ two central spikelets on either side ~~and~~ in the middle of each spike with *F. graminearum* strain PH-1 and 21 days later collected rachis and florets separately from ~~five equal sections of each~~ Morex and H369Y spikes (Figure 6A-C). Each spike was separated into five equal portions based on the total number of rachis nodes. Section 1 was on the base of the spike and section 5 at the tip. Section 3 contained the inoculated central spikelets, the lateral spikelets adjacent to the inoculated spikelets, and all central and lateral spikelets of the rachis nodes directly acro- and basipetal of the inoculated spikelets. For example, if the spike contained 60 spikelets, there were 12 spikelets and four rachis nodes in each section. For each section, ergosterol and DON accumulation was measured separately for floret and rachis tissue. Ergosterol is a major sterol found in fungal cell membranes and was used as a proxy for *F. graminearum* quantity. Ergosterol accumulation was significantly increased in section 4, located acropetal to the inoculated spikelets, of H369Y plants compared to wild-type Morex. H369Y plants also contained significantly more ergosterol in the rachis sections two and three compared to Morex (Figure 6A and C). DON levels were significantly higher in H369Y florets in sections two, three, and four as well as H369Y rachis in sections three and four (Figure 6B and C). We conclude that H369Y plants contain more DON and *F. graminearum* than wild-type Morex, specifically in the rachis near the inoculation site.

Next, we decided to study symptom development in H369Y and Morex plants upon inoculation with a *F. graminearum* reporter strain that constitutively expressed dsRed (*pgpdA::dsRed*) (Ilgen et al., 2009). For these experiments, we only inoculated one central floret in the middle of the spike and reduced the *F. graminearum* inoculum by half to reduce the

chance of mycelium development on the outside of the spike. Spread of FHB symptoms and overall FHB severity 14 days after inoculation were strongly increased in H369Y spikes compared to wild-type Morex (Supplemental Figure 11A-D). Increased FHB severity was observed after point inoculation of homozygous H369Y plants 7 and 21 days after inoculation, but not in corresponding sister lines (Supplemental Figure 11E). In T368I and H369Y mutant plants browning of the rachis was observed over the entire length of the rachis, but not in the corresponding wild-type sister lines. We used confocal laser scanning microscopy to visualize fungal mycelia at base of the spike and observed structures that resembled fungal hyphae in higher magnification images of both T368I and H369Y mutants plants, while no fungal signal was observed in the corresponding wild-type tissues (Figure 7A). Next confocal laser scanning microscopy was used to visualize the infection process in H369Y and Morex plants in more detail. While *F. graminearum* could be detected at the rachis nodes directly at the inoculated spikelets in both H369Y and Morex, *F. graminearum* was only detected at the fourth rachis nodes acro- and basipetal of the inoculated spikelets in H369Y, but not Morex (Figure 7B and Supplemental Figure 12). Additionally, *F. graminearum* was detected throughout the rachis node and all rachis tissue at the inoculated rachis node in H369Y. In contrast *F. graminearum* was detected only locally at the rachis node of the inoculated spikelet in wild-type rachis tissue and not in more distant parts of the rachis (Figure 7B and Supplemental Figure 12). This shows that *F. graminearum* does infect the rachis of H369Y plants, but is arrested at the inoculated rachis node in wild-type plants. Examination of the susceptible PI383933 plants showed a similar pattern to wild-type plants (Supplemental Figure 10C). We conclude, UGT13248-dependent detoxification of DON is required for type II resistance in barley.

DISCUSSION AND CONCLUSIONS

UGT13248 function in barley is highly conserved

Here, we screened 45 barley accessions for natural variation in full-length *UGT13248* (Supplemental Table 1) and 458 accessions for natural variation in two regions of *UGT13248*

covered by exome capture sequencing (Supplemental Table 2). The accessions tested include modern cultivars, landraces, and wild barleys. None of the 11 non-synonymous mutations identified, resulted in disruption of DON resistance in barley seedlings carrying these mutations (Supplemental Figures 1 and 4). Only one of these mutations, F385S, was located within the PSPG motif, thought to be required for UGT-UDP-sugar interaction (Supplemental Figure 3A). Further, protein modeling suggested that none of the mutations was likely to disrupt UGT13248 protein function (Supplemental Figures 2 and 3). Interestingly, the only UGT13248 mutations with reduced UGT13248 function were H369Y and T368I, found in a sodium azide-mutagenized TILLING population of barley cultivar Morex (Figure 1). We conclude that UGT13248 gene function is highly conserved in barley.

UGT13248 converts DON to D3G in barley

It has previously been shown that UGT13248 expression in yeast and wheat resulted in the conversion of DON to D3G (Li et al., 2015; Schweiger et al., 2010). Here, we observed that DON to D3G conversion in barley spikes that carried T368I and H369Y mutations was significantly reduced compared to wild-type barley (Figure 3B). We also demonstrated that constitutive expression of *UGT13248* under the control of the *Zea mays Ubiquitin* (Ubi1) promoter resulted in strongly increased DON to D3G conversion (Figure 3A). This further shows that UGT13248 catalyzes DON to D3G conversion *in planta*. While *UGT13248* expression was induced by DON treatment in both barley spikes with wild-type and constitutive *UGT13248* expression, low-level constitutive *UGT13248* expression was observed even in plants that did not carry the *Ubi-1*::*UGT13248* transgene (Supplemental Figure 5D). This suggests that *UGT13248* expression is upregulated upon DON application and that the level of *UGT13248* expression might be regulated by a feedback mechanism that prohibits continued *UGT13248* expression in response to DON after a certain *UGT13248* expression level is reached.

UGT13248 has been shown to catalyze NIV to NIV3G conversion in wheat (Li et al., 2017). Interestingly, *Arabidopsis* DOGT1 (UGT73C5) showed activity on DON and the growth hormone brassinolide, but not NIV (Poppenberger et al., 2005). Another Arabidopsis UGT,

UGT73C6, converted zearalenone to ZON-4-O-Glc in yeast (Poppenberger et al., 2006). The closest homolog to DOGT1 in barley UGT5876, did not show activity to DON in yeast (Schweiger et al., 2010). This shows that UGTs are promiscuous and might have multiple substrates. It is possible that UGT13248 can glucosylate other trichothecenes in barley, as well as potentially unrelated compounds including growth regulators and mycotoxins produced by other fungal pathogens. However, constitutive expression of UGT13248 did not lead to any detectable pleiotropic effects. Hence, it is unlikely that UGT13248 drastically affects plant growth regulation, as opposed to DOGT1 in *Arabidopsis* where overexpression plants showed a dwarf phenotype (Poppenberger et al., 2005).

UGT13248 is a major resistance factor in barley to *Fusarium graminearum*

Barley carrying mutations in UGT13248 that caused reduced UGT13248 function, H369Y and T368I, are highly susceptible to *F. graminearum*, both in field studies and in point inoculation experiments (Figures 4 and 5). The difference in FHB severity is clearest with point inoculation experiments (Figure 5). We conclude that UGT13248 is required for type II resistance to *F. graminearum* in barley. Our experiments cannot distinguish between type I and type II resistance in the field and we cannot rule out an additional effect of UGT13248 on type I resistance in field studies. The conserved type II resistance observed for this species (Steffenson, 2003) might be due to conserved UGT13248 function.

Previously, the *B. distachyon* UGT Bradi5g03300, the closest *Brachypodium* homolog to barley UGT13248, was suggested to not contribute to type II resistance in that species (Pasquet et al., 2016). Mutations in Bradi5g03300 only caused increased colonization with *F. graminearum* when spray inoculation was used. In contrast, point inoculation experiments did not show any difference in FHB severity between plants with mutations in Bradi5g03300 compared to wild-type plants (Pasquet et al., 2016). The mutations in Bradi5g03300 are located within the PSPG box similar to the H369Y and T368I mutations in barley UGT13248 studied here (Supplemental Figure 13). The observed differences may be due to differences in flower morphology in *B. distachyon* compared to barley. It is also possible that the study of

Bradi5g03300 was complicated by the presence of Bradi5g02780, another UGT that showed DON resistance in yeast (Schweiger et al., 2013), and that may be functionally redundant with Bradi5g03300. The differences observed in the function of UGTs in this study compared to *B. distachyon* show that studies in model organisms may not always be predictive of the mechanism observed in related crop species.

In wheat, a few major contributors to FHB resistance, including *Fhb1* and *Fhb7*, have been identified (Bai et al., 1999; Wang et al., 2020). However, in barley, FHB resistance has previously been found to be multifactorial and mainly dependent on agro-morphological traits (Massman et al., 2011). Hence, our identification of a major contributor to type II resistance in barley is notable. Interestingly, previous barley mapping studies have not identified a QTL associated with FHB resistance and coincident with *UGT13248*, which is likely due to functional conservation of UGT13248.

While barley UGT13248 was found to play a critical role in plant immunity to *F. graminearum*, it is curious why UGT13248 appears functionally conserved globally in barley, as not all growth regions are likely substantially affected by FHB outbreaks. However, various plant pathogenic fungi of the genera *Fusarium*, *Microcyclospora*, *Myrothecium*, *Peltaster*, *Spicellum*, *Stachybotrys*, *Trichoderma*, and *Trichothecium* produce trichothecene mycotoxins (Proctor et al., 2018). Up to 87% of tested food and feed samples from the Middle East and Africa contained type B trichothecenes (Rodrigues et al., 2011). It is possible that UGT13248 can detoxify trichothecene mycotoxins from various fungal pathogens and might hence contribute to disease resistance in many different environments. It can also not be ruled out that UGT13248 glucosylates other unknown compounds that are unrelated to trichothecenes.

Interestingly, in *Aegilops tauschii* nine of 147 accessions tested showed increased FHB susceptibility and increased FHB spread (Kirana et al., 2022). These nine accessions all carried a nonsense mutation just prior to the PSPG box in the UGT AET5Gv20385300 (Supplemental Figure 13), an ortholog of barley UGT13248 (Kirana et al., 2022). *A. tauschii* is the D subgenome donor for bread wheat and the sequenced cultivar Chinese Spring did also contain a missense mutation in the wheat ortholog of UGT13248 in the D genome (Kirana et al., 2022). This again

raises the question why UGT13248 is functionally conserved globally in barley but not in these related species.

DON detoxification is required for type II resistance to FHB in barley

Trichothecene production is known to be required for *Fusarium graminearum* spread in wheat spikes (Jansen et al., 2005; Schroeder and Christensen, 1963). In the barley cultivar 'Chevron',however, both wild-type and *tri5* mutant strains of *F. graminearum* were arrested at the rachis node of the inoculated spikelet (Jansen et al., 2005). Utilizing functional mutations in UGT13248, H369Y and T368I, we showed that functional UGT13248 is required for the arrest of *F. graminearum* at the inoculated rachis node in barley (Figure 7 and Supplemental Figures 11 and 12). Hence, the functional conservation of UGT13248 across barley may explain the conserved type II resistance observed for this species (Steffenson, 2003).

MATERIALS AND METHODS

Plant Material and growth conditions

Plants were grown at 20°C, 16 h daylight, and 8 h dark at 18°C in BM2 soil (Berger) with 3-4 seedlings per five-inch square pot. After seedling emergence, plants were fertilized with Osmocote plus fertilizer (Scotts). The plant genotypes used in this study are summarized in Table 1.

Transgenic barley plants

The *UGT13248* gene was previously cloned with a *C*-terminal FLAG tag into pENTR TM/ D TOPO (Shin et al., 2012) and transferred into binary vector pIPKb002 (Himmelbach et al., 2007) using Gateway cloning technology (Invitrogen). Immature barley cultivar Golden Promise embryos were transformed using the *Agrobacterium tumefaciens* strain AGL1 and transformants were selected on 50 mg / L hygromycin containing media (Hensel et al., 2008). T1 plants were screened for the presence of the transgene using UGT13248_fwd and FLAG_rev primers

(Supplemental Table 3). For DNA gel blotting genomic DNA (10 µg) was digested with XbaI, separated on a 1 % agarose gel, and transferred onto Hybond N+ membranes (Amersham Biosciences). The *hpt* gene probe was derived from a PCR-amplified product (Supplemental Table 3). The probe was labeled with α-^{32}P CTP using the Prime-a-Gene labeling system (Promega), following the manufacturer's instructions. The radiolabeled *hpt* probe was used for the hybridization, and results were visualized using autoradiography.

One transgenic plant each from two independent transgenic events was crossed to barley cultivar Rasmusson and F_1 plants were backcrossed to Rasmusson. In the F_3 generation, individuals containing the UGT13248-FLAG (UGT+) and individuals not containing the transgene (UGT-) were identified. All experiments were conducted using grains that descended from a single individual plant and were used in the BC_1F_6 generation.

For Western Blot analysis one individual seedling for each genotype was harvested and tissue was ground in liquid nitrogen. Plant tissue was mixed with equal volumes of 2 x Laemmli buffer, heated at 95°C for 5 minutes and supernatant was loaded onto a 10% polyacrylamide gel (Biorad, USA, 1610182). Stain-free technology was used to visualize equal loading of the gel. The proteins were transferred onto a PVDF membrane and Western Blot analysis was performed according to the manufacturer's instructions using an anti-FLAG HRP antibody (GenScript, USA, A01428).

TILLING lines

The TILLMore population (Talame et al., 2008a, b) of 4,906 M3 families in the background of the cv. Morex, mutagenized with NaN_3 was screened for mutations in *UGT13248* (Talame et al., 2008a, b). We identified three non-synonymous mutations in 2,432 families screened with four sets of primer pairs spanning exon 2 and the first 283 bp of exon 3. DNA samples of the TILLMore resource were organized in 8-fold pools and analysed by High Resolution Melting (HRM). With HRM, allelic differences are detected based on differences in melting temperature using a DNA intercalating dye. A 7500 FAST Real Time- HRM- ready instrument (Applied Biosystems) was used, along with Melt Doctor Amplification kit (Applied Biosystems). HRM

primers were designed based on the UGT13248 sequence (GenBank GU170355). Primers are listed in Supplemental Table 3. Putative mutants were confirmed by Sanger sequencing using a TILLING_fwd and TILLING_rev primers (Supplemental Table 3). Three lines carrying mutations in UGT13248 were identified. TILLMore #438 contained a C to T nucleotide substitution at base pair 1103 of the cDNA sequence that caused a T368I amino acid substitution of UGT13248. TILLMore #1624 carried a G to A nucleotide substitution at bp 1105 of the cDNA sequence, resulting in a S403N amino acid substitution. TILLMore #1683 carried a C to T nucleotide substitution at 1208 bp, resulting in a H369Y amino acid substitution. Homozygous plants were used in the M6/ M7 generation. For Supplemental Figure 6, M6 plants were crossed with Morex and progeny in the BC_1F_2 generation was used. Sister lines that contained the homozygous mutant or wild-type allele, respectively, were selected for T368I and H369Y in the BC_4F_2 generation. We only selected lines with a 6-row morphology. These lines were used for Figure 6A and Supplemental Figure 11E.

Full-length sequencing of UGT13248

Genomic DNA from 26 barley genotypes (Supplemental Table S1, all genotypes from Huang *et al.*, 2013) was extracted using the Plant/Fungi DNA Isolation Kit (Norgen Biotek). Sanger sequencing was performed with primer sets designed to cover 2,477 bp of *UGT13248* genomic sequence (Table S3). Genomic sequences of UGT13248 from 19 additional accessions were obtained from Jayakodi *et al.* (2020) (Jayakodi et al., 2020) (Jayakodi et al., 2020). Sequences were compared using BLAST (https://blast.ncbi.nlm.nih.gov).

Exome capture resequencing data collection and processing

All resequencing data reported here are derived from previously published datasets, including wild, landrace, and elite barley lines reported in (Chen et al., 2022; Hemshrot et al., 2019; Kono et al., 2019; Lei et al., 2019; Mascher et al., 2013; Nice et al., 2016; Russell et al., 2016). The sequence was generated after exome capture using the barley Roche NimbleGen (Madison, WI) SeqCap EZ Developer probe pools (Mascher et al., 2013).

For sequence alignment and quality control, we used publicly available software integrated with bash scripts in the "sequence_handling" workflow (Liu et al., 2022). Sequence quality assessment used FastQC (http://www.bioinformatics.bbsrc.ac.uk/projects/fastqc/). Adapters were trimmed using Scythe (https://github.com/vsbuffalo/scythe). Burrows-Wheeler Aligner (BWA-MEM) (Li et al., 2009) was used to align reads to the barley reference genome Morex_v2 (Monat et al., 2019). Read mapping used default parameters for BWA-MEM except for the following: 16 threads, minimum seed length of 8, re-seed value of 1.0, gap penalty of 8, and a minimum threshold of 85 for 100 bp PE reads or a minimum threshold of 106 for 125 bp PE reads. Read mapping parameters were chosen to permit a ~2% mismatch between reads and the reference sequence; the highest estimated nucleotide diversity reported based on Sanger resequencing in wild and cultivated barley (Morrell et al., 2014; Morrell et al., 2003; Morrell et al., 2006). Picard v2.20.2 (https://github.com/broadinstitute/picard), was used for alignment sorting, de-duplicating, and adding read groups to the read-mapped files. Read depth, and coverage estimates were generated by 'bedtools genomecov' (Quinlan and Hall, 2010). We used ~241X exome capture reads from a Morex sample (Mascher et al., 2013) to the Morex v2 reference genome empirically define regions are considered covered by exome capture (https://github.com/MorrellLAB/captured_50x_BED). These (Quinlan and Hall, 2010) "cap50x" have > 50X coverage in Morex capture data (https://github.com/MorrellLAB/captured_50x_BED).

Alignment processing followed the Genome Analysis Toolkit (GATK) best practices workflow (DePristo et al., 2011; McKenna et al., 2010). Individual sample genotype likelihoods were then calculated using GATK v4.1.2 HaplotypeCaller, with a value of 0.008 per base pair passed to the "heterozygosity" option. This value is the mean estimate of coding nucleotide sequence diversity, based on previous Sanger resequencing experiments (Caldwell et al., 2006; Morrell et al., 2014). Single sample GVCFs were merged using GenomicsDBImport, then called jointly from the genotype likelihoods with the GATK tool Genotype GVCFs (McKenna et al., 2010). GATK's Variant Quality Score Recalibration (VQSR) was used for variant filtering. SNPs were also filtered to include sites that fall within the "cap50x" regions**,** are polymorphic and bi-allelic with genotype quality (GQ) > 3, and have per sample depth (DP) between 5 and 78

(extremely high depth is likely due high copy number genomic regions collapsed in the reference genome, so we take the 95th percentile of coverage as the upper cutoff). Heterozygous genotypes were set to missing if the allele balance deviated more than 0.1 from the expected allele balance of 0.5 (Muyas et al., 2019; Pedersen et al., 2021). Briefly, allele balance helps identify systematic or alignment errors that could result in false SNP calls. The filtered VCF was generated as part of a larger cohort of samples with 458 of the samples used for this study. Genotyping for the UGT13248 locus was extracted from the GATK-derived VCF using bcftools (Danecek et al., 2021) (https://github.com/MorrellLAB/Locus_HvUGT13248).

UGT13248 CDS according to Morex V2 starting position is Chr5 position 330626689.

Plant height, spike length and spike density

Height was measured as the distance from the base of the plant to the top of the spike, excluding awns on eight plants each. Spike length was measured as the distance between the top and bottom spikelets on five spikes. Spike density was calculated as the number of rachis nodes per cm spike.

DON plate assays, DON inoculation, and DON and D3G measurements

Barley grains were surface-sterilized for 10 minutes in a 1 % sodium hypochlorite solution containing 0.01 % Tween 20. Grains were washed five times with sterile water and placed on ½ x Murashige and Skoog (MS) medium with 0.8 % agar. Plates were kept at 4 °C for two days for stratification and then transferred to 16 h light / 8 h dark conditions at 22 °C for two to three days. Seedlings were transferred onto ½ x MS medium containing 1 mg / L DON or mock. DON was dissolved in 70 % ethanol at 5 mg / mL and stored at -20°C. Five mg / mL DON stock solution was added at 1:5000 ratio to medium for 1 mg / mL DON plates. Similarly, 70 % ethanol was added at 1:5000 ratio to medium for mock plates. Root length was measured daily for six days.

For inoculation experiments, DON was diluted to 0.2 µg / µL, and 10 µL of this solution were inoculated at anthesis between the palea and lemma of each floret. We inoculated three

central spikelets on each side of any spike and harvested the inoculated section of the spike (total of 18 spikelets). For each biological replicates spike sections from three separate spikes were combined. Samples were ground in liquid nitrogen and trichothecenes extracted with 4 volumes per weight with a mixture of acetonitrile /water /acetic acid: 79 / 20 / 1 for 90 minutes at room temperature. 500 µL per sample were dried down and resuspended in 1 mL 50 % aqueous methanol, centrifuged and transferred into HPLC vials and measured using a 1290 Agilent UHPC system coupled to a Sciex 6500+ QTrap MS. Liquid chromatography and tandem mass spectrometry details were as previously described (Fiby et al., 2021).

For Figure 6A and B, DON was measured in parts per million (µg / g), by gas chromatography/mass spectrometry (Mirocha et al., 1998). Ergosterol was measured as described previously (Dong et al., 2006). Samples that were below the detection limit were set to 0 mg / L.

Plant inoculation *with F. graminearum*

F. graminearum was grown in liquid CMC medium (15g / L carboxymethylcellulose (CMC), 1 g / L NH_4NO_3, 1 g / L KH_2PO_4, 0.5 g / L $MgSO_4$ x 7 H_2O and 1 g / L Yeast Extract) for five days at room temperature while shaking at 150 rpm. Fungal cultures were filtered through 1-fold Miracloth, and filtrate was collected by centrifugation for 10 minutes at 2500 x *g* and 4 ˚C. Fungal spores were washed with sterile water and the concentration was adjusted to 1 x 10^8 macroconidia per mL.

For point inoculation experiments with *F. graminearum* strain PH-1, one central spikelet in the middle of each side of a spike was inoculated with 10 µl *F. graminearum* (PH 1) at 1 x 10^5 macroconidia / mL at anthesis in a controlled environment chamber. Inoculated spikes were covered with a plastic bag for 48 h. FHB severity was scored at the indicated time points by calculating the ratio of the number of infected spikelets versus the total number of spikelets.

For field experiments each genotype was planted in a 1.52 m × 0.31 m single-row plot and inoculation experiments were performed as previously described (Huang et al., 2021). In brief Morex, T368I, H369Y, and S403N genotypes were planted in six replicates for each

location (Saint Paul and Crookston) and year (2019 and 2020). The susceptible check Stander and the resistant check Chevron were planted in 3 replicates for each location and year. In Saint Paul, plants were spray-inoculated twice with 1×10^5 macroconidia / mL *F. graminearum* within three to four days. The first application was performed two days after heading. In Crookston, plants were inoculated by spreading *F. graminearum*-colonized maize seed (grain spawn) onto the soil surface at the four–five leaf stage and at flag-leaf emergence. Mist irrigation was used from before the first inoculation and maintained until FHB severity was recorded to facilitate disease development. FHB severity was scored by calculating the ratio of the counted number of infected kernels versus the total number of kernels within a spike from ten randomly selected spikes per plot. For each plot, the ratios were averaged to obtain FHB severity for each biological replicate. DON was measured on grain samples harvested from FHB nurseries in Saint Paul after threshing and cleaning. A sample of cleaned grains from each plot was measured for DON accumulation, in parts per million (µg / g), by gas chromatography/mass spectrometry as previously described (Mirocha et al., 1998).

Protein modeling

Structural models of UGT13248 were created using SWISS-MODEL (Waterhouse et al., 2018). Protein BLAST searches were conducted within the SWISS-MODEL server. The protein sequence submitted for BLAST searches was METTVTAVSGTTSSSVGHGAGGGAARVLLLPSPGAQGHTNPMLQLGRRLAYHGLRPTLVATRYVLSTTPAPGAPFDV AAISDGFDAGGMALCPDPAEYFSRLEAVGSETLRELLLSEARAGRPVRVLVYDAHLAWARRVAQASGVAAAAFFSQPC SVDVVYGELWAGRLALPATDGRALLARGVLGVELGLEDMPPFAAVPESQPAFLQVSVGQFEGLDYADDVLVNSFRDIE PKEVEYMELTWRAKMVGPTLPSYYLGDGRLPSNKSYGLDLFNSEVECMDWLEKQMNSSVVLVSYGTVSNYDATQLEE LGNGLCNSSKPFLWVVRSNEEHKLSEELKEKCGKIGLIVSWCPQLEVLAHRAIGCFVTHCGWNSTLEALVNGVPFVGIPH WADQPTIAKYVESAWGMGVRARKNKNGCLKKEEVERCIREVMDGERKDEYKKNAMNWMQKAKEAMQEGGSSDK HVAEFATKYSSI. The template with the highest sequence identity was selected for modeling (73 % sequence identity). The model was built using the three-dimensional crystal structure of *Os*79 in complex with the non-reactive co-substrate UDP-2-fluoro-2-deoxy-D-glucose and trichothecene (PDB ID: 5TMD) (Wetterhorn et al., 2016) as the search template. Structural

models were visualized in the PyMOL Molecular Graphics System, Version 1.2r3pre (Schrödinger, LLC) to determine putative active site motifs. Putative ligand non-reactive mimic UDP-2-fluoro-2-deoxy-D-glucose and trichothecene were docked in the active site by structural alignment. Structural models of UGT13248 mutants were generated and compared in PyMOL (Barber, 2021).

Confocal Microscopy

A *F. graminearum* reporter strain 8/1 with constitutive dsRed expression (*pgpdA::dsRed*) and inducible GFP expression (*pTRI5::GFP*) (Ilgen et al., 2009) was used to monitor fungal growth and trichothecene biosynthesis *in vivo*. Five µl of a 1 x 10^5 macroconidia / mL suspension was applied to one central floret on one side of the spike and covered with clear plastic bag for 24 hours to maintain high humidity. At 14 dpi, rachises of infected barley spikes were hand-sectioned longitudinally and observed using confocal laser scanning microscopy (Nikon A1si, UMN Imaging Center). Optical configuration for fluorescence detection was as previously described (Boenisch and Schäfer, 2011). Plant cell wall autofluorescence (DAPI) was excited at 406 nm and detected in the 425-475 nm range. DsRed was excited at 562 nm and detected in the 575-625 nm range. Z-stacking was used to collect images at multiple focal planes. Image processing and data generation were performed using the Nikon NIS-Elements platform (www.microscope.healthcare.nikon.com/products/software/nis-elements).

ACKNOWLEDGEMENTS

We thank Sean O'Mara (UMN) for preparing fungal inoculum and help with inoculations, Ruth Dill-Mackey's research group (UMN) for preparing fungal inoculum for field experiments, Wilhelm Schäfer (University of Hamburg, Germany) for the *F. graminearum* reporter strain (Ilgen et al., 2009), Nils Stein (IPK Gatersleben, Germany), and Brian Steffenson (UMN) for barley accessions used in this manuscript and Bruna Bucciarelli (UMN) for help with formatting Confocal Laser Scanning Microscopy images. The excellent technical assistance of Carola Bollmann (IPK Gatersleben, Germany) for generating transgenic barley is acknowledged. This

work was supported by the resources and staff at the University of Minnesota University Imaging Centers (UIC) SCR_020997. This work was funded by the Endowment in Molecular Genetics Applied to Crop Improvement at the University of Minnesota and the United States Department of Agriculture, under Agreement No. 59-0206-4-140 and 59-0206-4-135. This is a cooperative project with the United States Wheat and Barley Scab Initiative. Any opinions, findings, conclusions, or recommendations expressed in this publication are those of the authors and do not necessarily reflect the view of the United States Department of Agriculture.

AUTHOR CONTRIBUTIONS

G.B. and G.J.M. designed the research. G.B., Y.H., G.H., S.H., X.L., M.Q., Y.D., and F.B. performed research. S.M., S.S. and J.K. provided tools. G.B., Y.H., C.L., S.R.W., and P.L.M. analyzed data. G.B. wrote the paper with input from all authors.

SUPPLEMENTAL MATERIALS

Supplemental Table 1: List of accessions used for full-length sequencing of *UGT13248*.

Supplemental Table 2: List of accessions used for exome capture sequencing analysis.

Supplemental Table 3: List of primers.

Supplemental Figure 1: Non-synonymous mutations identified in *UGT13248* in 45 barley accessions.

Supplemental Figure 2: Comparison of rice Os79 and barley UGT13248.

Supplemental Figure 3: Non-synonymous mutations identified using exome capture sequencing of 458 barley accessions.

Supplemental Figure 4: Seedling root growth upon treatment with DON.

Supplemental Figure 5: UGT13248 overexpression lines.

Supplemental Figure 6: The wild-type *UGT13248* gene is a single dominant gene that confers seedling root resistance to DON.

Supplemental Figure 7: Plant height, DON and D3G measurements in field experiments.

Supplemental Figure 8: Plant Height and spike density for UGT13248 overexpression lines.

Supplemental Figure 9: Only H369Y and PI383933 plants show increased FHB severity in point inoculation experiments.

Supplemental Figure 10: Susceptibility of PI383933 is not due to mutations in UGT13248.

Supplemental Figure 11: Disease symptoms after point inoculation with *F. graminearum* reporter strain.

Supplemental Figure 12: *F. graminearum* reporter strain is detected in H369Y rachis tissue.

Supplemental Figure 13: Alignment of orthologous UGT sequences in rice (Os79), barley (UGT13248), *B. distachyon* (Bradi5g03300), *Aegilops tauschii* (AET5Gv20385300) and wheat (*Ta*UGT5D).

REFERENCES

Bai, G.H., Kolb, F.L., Shaner, G., and Domier, L.L. (1999). Amplified fragment length polymorphism markers linked to a major quantitative trait locus controlling scab resistance in wheat. Phytopathology *89*, 343-348.

Bai, G.H., Plattner, R., Desjardins, A., and Kolb, F. (2001). Resistance to Fusarium head blight and deoxynivalenol accumulation in wheat. Plant Breeding *120*, 1-6.

Bai, G.H., Su, Z.Q., and Cai, J. (2018). Wheat resistance to Fusarium head blight. Can J Plant Pathol *40*, 336-346.

Barber, R.D. (2021). Software to Visualize Proteins and Perform Structural Alignments. Curr Protoc *1*, e292.

Boddu, J., Cho, S., Kruger, W.M., and Muehlbauer, G.J. (2006). Transcriptome analysis of the barley-Fusarium graminearum interaction. Mol Plant Microbe In *19*, 407-417.

Boddu, J., Cho, S.H., and Muehlbauer, G.J. (2007). Transcriptome analysis of trichothecene-induced gene expression in barley. Mol Plant Microbe In *20*, 1364-1375.

Boenisch, M.J., and Schäfer, W. (2011). Fusarium graminearum forms mycotoxin producing infection structures on wheat. Bmc Plant Biol *11*.

Bushnell, W.R., Hayen, B.E., and Pritsch, C. (2003). Histology abd Physiology of Fusarium head blight. In Fusarium head blight of wheat and barley, K.J. Leonard, and W.R. Bushnell, eds. (St. Paul, MN, USA, American Phytopathological Society Press), pp. 44-83.

Caldwell, K.S., Russell, J., Langridge, P., and Powell, W. (2006). Extreme population-dependent linkage disequilibrium detected in an inbreeding plant species, Hordeum vulgare. Genetics *172*, 557-567.
Chen, Y., Kistler, H.C., and Ma, Z.H. (2019). Fusarium graminearum Trichothecene Mycotoxins: Biosynthesis, Regulation, and Management. Annual Review of Phytopathology, Vol 57, 2019 *57*, 15-39.
Chen, Y.Y., Schreiber, M., Bayer, M.M., Dawson, I.K., Hedley, P.E., Lei, L., Akhunova, A., Liu, C.C., Smith, K.P., Fay, J.C*., et al.* (2022). The evolutionary patterns of barley pericentromeric chromosome regions, as shaped by linkage disequilibrium and domestication. Plant J *111*, 1580-1594.
Danecek, P., Bonfield, J.K., Liddle, J., Marshall, J., Ohan, V., Pollard, M.O., Whitwham, A., Keane, T., McCarthy, S.A., Davies, R.M*., et al.* (2021). Twelve years of SAMtools and BCFtools. Gigascience *10*.
de la Peña, R.C., Smith, K.P., Capettini, F., Muehlbauer, G.J., Gallo-Meagher, M., Dill-Macky, R., Somers, D.A., and Rasmusson, D.C. (1999). Quantitative trait loci associated with resistance to Fusarium head blight and kernel discoloration in barley. Theor Appl Genet *99*, 561-569.
DePristo, M.A., Banks, E., Poplin, R., Garimella, K.V., Maguire, J.R., Hartl, C., Philippakis, A.A., del Angel, G., Rivas, M.A., Hanna, M*., et al.* (2011). A framework for variation discovery and genotyping using next-generation DNA sequencing data. Nat Genet *43*, 491-+.
Dong, Y., Steffenson, B.J., and Mirocha, C.J. (2006). Analysis of ergosterol in single kernel and ground grain by gas chromatography-mass spectrometry. J Agric Food Chem *54*, 4121-4125.
Evans, C.K., Xie, W., Dill-Macky, R., and Mirocha, C.J. (2000). Biosynthesis of deoxynivalenol in spikelets of barley inoculated with macroconidia of Fusarium graminearum. Plant Disease *84*, 654-660.
Ferrigo, D., Raiola, A., and Causin, R. (2016). Fusarium Toxins in Cereals: Occurrence, Legislation, Factors Promoting the Appearance and Their Management. Molecules *21*.
Fiby, I., Sopel, M.M., Michlmayr, H., Adam, G., and Berthiller, F. (2021). Development and Validation of an LC-MS/MS Based Method for the Determination of Deoxynivalenol and Its Modified Forms in Maize. Toxins *13*.
Gachon, C.M.M., Langlois-Meurinne, M., and Saindrenan, P. (2005). Plant secondary metabolism glycosyltransferases: the emerging functional analysis. Trends in Plant Science *10*, 542-549.
Gardiner, S.A., Boddu, J., Berthiller, F., Hametner, C., Stupar, R.M., Adam, G., and Muehlbauer, G.J. (2010). Transcriptome Analysis of the Barley-Deoxynivalenol Interaction: Evidence for a Role of Glutathione in Deoxynivalenol Detoxification. Mol Plant Microbe In *23*, 962-976.
He, Y., Wu, L., Liu, X., Jiang, P., Yu, L.X., Qiu, J.B., Wang, G., Zhang, X., and Ma, H.X. (2020). TaUGT6, a Novel UDP-Glycosyltransferase Gene Enhances the Resistance to FHB and DON Accumulation in Wheat. Front Plant Sci *11*.
Hemshrot, A., Poets, A.M., Tyagi, P., Lei, L., Carter, C.K., Hirsch, C.N., Li, L., Brown-Guedira, G., Morrell, P.L., Muehlbauer, G.J*., et al.* (2019). Development of a Multiparent Population for Genetic Mapping and Allele Discovery in Six-Row Barley. Genetics *213*, 595-613.
Hensel, G., Valkov, V., Middlefell-Williams, J., and Kumlehn, J. (2008). Efficient generation of transgenic barley: the way forward to modulate plant-microbe interactions. J Plant Physiol *165*, 71-82.
Himmelbach, A., Zierold, U., Hensel, G., Riechen, J., Douchkov, D., Schweizer, P., and Kumlehn, J. (2007). A set of modular binary vectors for transformation of cereals. Plant Physiol *145*, 1192-1200.
Hohn, T.M., and Beremand, P.D. (1989). Isolation and Nucleotide-Sequence of a Sesquiterpene Cyclase Gene from the Trichothecene-Producing Fungus Fusarium-Sporotrichioides. Gene *79*, 131-138.
Huang, Y., Haas, M., Heinen, S., Steffenson, B.J., Smith, K.P., and Muehlbauer, G.J. (2018). QTL Mapping of Fusarium Head Blight and Correlated Agromorphological Traits in an Elite Barley Cultivar Rasmusson. Front Plant Sci *9*, 1260.
Huang, Y.D., Millett, B.P., Beaubien, K.A., Dahl, S.K., Steffenson, B.J., Smith, K.P., and Muehlbauer, G.J. (2013). Haplotype diversity and population structure in cultivated and wild barley evaluated for Fusarium head blight responses. Theor Appl Genet *126*, 619-636.

Huang, Y.D., Yin, L., Sallam, A.H., Heinen, S., Li, L., Beaubien, K., Dill-Macky, R., Dong, Y.H., Steffenson, B.J., Smith, K.P*., et al.* (2021). Genetic dissection of a pericentromeric region of barley chromosome 6H associated with Fusarium head blight resistance, grain protein content and agronomic traits. Theor Appl Genet *134*, 3963-3981.

Ilgen, P., Hadeler, B., Maier, F.J., and Schafer, W. (2009). Developing kernel and rachis node induce the trichothecene pathway of Fusarium graminearum during wheat head infection. Mol Plant Microbe Interact *22*, 899-908.

Jansen, C., von Wettstein, D., Schafer, W., Kogel, K.H., Felk, A., and Maier, F.J. (2005). Infection patterns in barley and wheat spikes inoculated with wild-type and trichodiene synthase gene disrupted Fusarium graminearum. Proc Natl Acad Sci U S A *102*, 16892-16897.

Jayakodi, M., Padmarasu, S., Haberer, G., Bonthala, V.S., Gundlach, H., Monat, C., Lux, T., Kamal, N., Lang, D., Himmelbach, A*., et al.* (2020). The barley pan-genome reveals the hidden legacy of mutation breeding. Nature *588*, 284-289.

Johns, L.E., Bebber, D.P., Gurr, S.J., and Brown, N.A. (2022). Emerging health threat and cost of Fusarium mycotoxins in European wheat. Nat Food *3*, 1014-+.

Kirana, R.P., Gaurav, K., Arora, S., Wiesenberger, G., Doppler, M., Michel, S., Zimmerl, S., Matic, M., Eze, C.E., Kumar, M*., et al.* (2022). Identification of a UDP-glucosyltransferase conferring deoxynivalenol resistance in Aegilops tauschii and wheat. Plant Biotechnology Journal.

Kono, T.J.Y., Liu, C., Vonderharr, E.E., Koenig, D., Fay, J.C., Smith, K.P., and Morrell, P.L. (2019). The Fate of Deleterious Variants in a Barley Genomic Prediction Population. Genetics *213*, 1531-1544.

Lee, H.J., and Ryu, D. (2017). Worldwide Occurrence of Mycotoxins in Cereals and Cereal-Derived Food Products: Public Health Perspectives of Their Co-occurrence. J Agric Food Chem *65*, 7034-7051.

Lei, L., Poets, A.M., Liu, C.C., Wyant, S.R., Hoffman, P.J., Carter, C.K., Shaw, B.G., Li, X., Muehlbauer, G.J., Katagiri, F*., et al.* (2019). Environmental Association Identifies Candidates for Tolerance to Low Temperature and Drought. G3-Genes Genom Genet *9*, 3423-3438.

Lemmens, M., Scholz, U., Berthiller, F., Dall'Asta, C., Koutnik, A., Schuhmacher, R., Adam, G., Buerstmayr, H., Mesterhazy, A., Krska, R*., et al.* (2005). The ability to detoxify the mycotoxin deoxynivalenol colocalizes with a major quantitative trait locus for fusarium head blight resistance in wheat. Mol Plant Microbe In *18*, 1318-1324.

Li, H., Handsaker, B., Wysoker, A., Fennell, T., Ruan, J., Homer, N., Marth, G., Abecasis, G., Durbin, R., and Proc, G.P.D. (2009). The Sequence Alignment/Map format and SAMtools. Bioinformatics *25*, 2078-2079.

Li, X., Michlmayr, H., Schweiger, W., Malachova, A., Shin, S., Huang, Y.D., Dong, Y.H., Wiesenberger, G., McCormick, S., Lemmens, M*., et al.* (2017). A barley UDP-glucosyltransferase inactivates nivalenol and provides Fusarium Head Blight resistance in transgenic wheat. Journal of Experimental Botany *68*, 2187-2197.

Li, X., Shin, S., Heinen, S., Dill-Macky, R., Berthiller, F., Nersesian, N., Clemente, T., McCormick, S., and Muehlbauer, G.J. (2015). Transgenic Wheat Expressing a Barley UDP-Glucosyltransferase Detoxifies Deoxynivalenol and Provides High Levels of Resistance to Fusarium graminearum. Mol Plant Microbe In *28*, 1237-1246.

Liu, C., Hoffman, P.J., Wyant, S.R., Dittmar, E.L., Takebasahi, N., Hamann, S., Lei, L., and Morrell, P.L. (2022). MorrellLAB/sequence_handling: Release v3.0: SNP calling with GATK 4.1 and Slurm compatibility.

Mascher, M., Richmond, T.A., Gerhardt, D.J., Himmelbach, A., Clissold, L., Sampath, D., Ayling, S., Steuernagel, B., Pfeifer, M., D'Ascenzo, M*., et al.* (2013). Barley whole exome capture: a tool for genomic research in the genus Hordeum and beyond. Plant J *76*, 494-505.

Massman, J., Cooper, B., Horsley, R., Neate, S., Dill-Macky, R., Chao, S., Dong, Y., Schwarz, P., Muehlbauer, G.J., and Smith, K.P. (2011). Genome-wide association mapping of Fusarium head blight resistance in contemporary barley breeding germplasm. Molecular Breeding *27*, 439-454.

Mayer, K.F.X., Waugh, R., Langridge, P., Close, T.J., Wise, R.P., Graner, A., Matsumoto, T., Sato, K., Schulman, A., Muehlbauer, G.J*., et al.* (2012). A physical, genetic and functional sequence assembly of the barley genome. Nature *491*, 711-+.

McCormick, S.P., Stanley, A.M., Stover, N.A., and Alexander, N.J. (2011). Trichothecenes: From Simple to Complex Mycotoxins. Toxins *3*, 802-814.

McKenna, A., Hanna, M., Banks, E., Sivachenko, A., Cibulskis, K., Kernytsky, A., Garimella, K., Altshuler, D., Gabriel, S., Daly, M*., et al.* (2010). The Genome Analysis Toolkit: A MapReduce framework for analyzing next-generation DNA sequencing data. Genome Res *20*, 1297-1303.

McLaughlin, C.S., Vaughn, M.H., Campbell, J.M., Wei, C.M., Stafford, M.E., and Hansin, B.S., eds. (1977). Inhibition of protein synthesis by trichothecenes. (Park Forest South, IL, U.S.A., Pathotoxin Publishers).

Mesfin, A., Smith, K.P., Dill-Macky, R., Evans, C.K., Waugh, R., Gustus, C.D., and Muehlbauer, G.J. (2003). Quantitative trait loci for fusarium head blight resistance in barley detected in a two-rowed by six-rowed population. Crop Sci *43*, 307-318.

Michlmayr, H., Varga, E., Lupi, F., Malachova, A., Hametner, C., Berthiller, F., and Adam, G. (2017). Synthesis of Mono- and Di-Glucosides of Zearalenone and alpha-/beta-Zearalenol by Recombinant Barley Glucosyltransferase HvUGT14077. Toxins *9*.

Mirocha, C.J., Kolaczkowski, E., Xie, W.P., Yu, H., and Jelen, H. (1998). Analysis of deoxynivalenol and its derivatives (batch and single kernel) using gas chromatography mass spectrometry. J Agr Food Chem *46*, 1414-1418.

Monat, C., Padmarasu, S., Lux, T., Wicker, T., Gundlach, H., Himmelbach, A., Ens, J., Li, C.D., Muehlbauer, G.J., Schulman, A.H*., et al.* (2019). TRITEX: chromosome-scale sequence assembly of Triticeae genomes with open-source tools. Genome Biology *20*.

Morrell, P.L., Gonzales, A.M., Meyer, K.K.T., and Clegg, M.T. (2014). Resequencing Data Indicate a Modest Effect of Domestication on Diversity in Barley: A Cultigen With Multiple Origins. J Hered *105*, 253-264.

Morrell, P.L., Lundy, K.E., and Clegg, M.T. (2003). Distinct geographic patterns of genetic diversity are maintained in wild barley (Hordeum vulgare ssp spontaneum) despite migration. P Natl Acad Sci USA *100*, 10812-10817.

Morrell, P.L., Toleno, D.M., Lundy, K.E., and Clegg, M.T. (2006). Estimating the contribution of mutation, recombination and gene conversion in the generation of haplotypic diversity. Genetics *173*, 1705-1723.

Muyas, F., Bosio, M., Puig, A., Susak, H., Domenech, L., Escaramis, G., Zapata, L., Demidov, G., Estivill, X., Rabionet, R*., et al.* (2019). Allele balance bias identifies systematic genotyping errors and false disease associations. Hum Mutat *40*, 115-126.

Nice, L.M., Steffenson, B.J., Brown-Guedira, G.L., Akhunov, E.D., Liu, C., Kono, T.J.Y., Morrell, P.L., Blake, T.K., Horsley, R.D., Smith, K.P*., et al.* (2016). Development and Genetic Characterization of an Advanced Backcross-Nested Association Mapping (AB-NAM) Population of Wild x Cultivated Barley. Genetics *203*, 1453-+.

Pasquet, J.C., Changenet, V., Macadre, C., Boex-Fontvieille, E., Soulhat, C., Bouchabke-Coussa, O., Dalmais, M., Atanasova-Penichon, V., Bendahmane, A., Saindrenan, P*., et al.* (2016). A Brachypodium UDP-Glycosyltransferase Confers Root Tolerance to Deoxynivalenol and Resistance to Fusarium Infection. Plant Physiol *172*, 559-574.

Pedersen, B.S., Brown, J.M., Dashnow, H., Wallace, A.D., Velinder, M., Tristani-Firouzi, M., Schiffman, J.D., Tvrdik, T., Mao, R., Best, D.H*., et al.* (2021). Effective variant filtering and expected candidate variant yield in studies of rare human disease. Npj Genom Med *6*.

Poppenberger, B., Berthiller, F., Bachmann, H., Lucyshyn, D., Peterbauer, C., Mitterbauer, R., Schuhmacher, R., Krska, R., Glossl, J., and Adam, G. (2006). Heterologous expression of Arabidopsis UDP-glucosyltransferases in Saccharomyces cerevisiae for production of zearalenone-4-O-glucoside. Appl Environ Microb *72*, 4404-4410.

Poppenberger, B., Berthiller, F., Lucyshyn, D., Sieberer, T., Schuhmacher, R., Krska, R., Kuchler, K., Glossl, J., Luschnig, C., and Adam, G. (2003). Detoxification of the Fusarium mycotoxin deoxynivalenol by a UDP-glucosyltransferase from Arabidopsis thaliana. J Biol Chem *278*, 47905-47914.

Poppenberger, B., Fujioka, S., Soeno, K., George, G.L., Vaistij, F.E., Hiranuma, S., Seto, H., Takatsuto, S., Adam, G., Yoshida, S.*, et al.* (2005). The UGT73C5 of Arabidopsis thaliana glucosylates brassinosteroids. P Natl Acad Sci USA *102*, 15253-15258.

Proctor, R.H., Hohn, T.M., and McCormick, S.P. (1995). Reduced virulence of Gibberella zeae caused by disruption of a trichothecene toxin biosynthetic gene. Mol Plant Microbe Interact *8*, 593-601.

Proctor, R.H., McCormick, S.P., Kim, H.S., Cardoza, R.E., Stanley, A.M., Lindo, L., Kelly, A., Brown, D.W., Lee, T., Vaughan, M.M.*, et al.* (2018). Evolution of structural diversity of trichothecenes, a family of toxins produced by plant pathogenic and entomopathogenic fungi. Plos Pathog *14*.

Quinlan, A.R., and Hall, I.M. (2010). BEDTools: a flexible suite of utilities for comparing genomic features. Bioinformatics *26*, 841-842.

Rodrigues, I., Handl, J., and Binder, E.M. (2011). Mycotoxin occurrence in commodities, feeds and feed ingredients sourced in the Middle East and Africa. Food Addit Contam B *4*, 168-179.

Russell, J., Mascher, M., Dawson, I.K., Kyriakidis, S., Calixto, C., Freund, F., Bayer, M., Milne, I., Marshall-Griffiths, T., Heinen, S.*, et al.* (2016). Exome sequencing of geographically diverse barley landraces and wild relatives gives insights into environmental adaptation. Nat Genet *48*, 1024-+.

Santini, A., Meca, G., Uhlig, S., and Ritieni, A. (2012). Fusaproliferin, beauvericin and enniatins: occurrence in food - a review. World Mycotoxin J *5*, 71-81.

Schroeder, H.W., and Christensen, J.J. (1963). Factors Affecting Resistance of Wheat to Scab Caused by Gibberella Zeae. Phytopathology *53*, 831-&.

Schweiger, W., Boddu, J., Shin, S., Poppenberger, B., Berthiller, F., Lemmens, M., Muehlbauer, G.J., and Adam, G. (2010). Validation of a candidate deoxynivalenol-inactivating UDP-glucosyltransferase from barley by heterologous expression in yeast. Mol Plant Microbe Interact *23*, 977-986.

Schweiger, W., Steiner, B., Ametz, C., Siegwart, G., Wiesenberger, G., Berthiller, F., Lemmens, M., Jia, H.Y., Adam, G., Muehlbauer, G.J.*, et al.* (2013). Transcriptomic characterization of two major Fusarium resistance quantitative trait loci (QTLs), Fhb1 and Qfhs.ifa-5A, identifies novel candidate genes. Mol Plant Pathol *14*, 772-785.

Shin, S., Torres-Acosta, J.A., Heinen, S.J., McCormick, S., Lemmens, M., Paris, M.P., Berthiller, F., Adam, G., and Muehlbauer, G.J. (2012). Transgenic Arabidopsis thaliana expressing a barley UDP-glucosyltransferase exhibit resistance to the mycotoxin deoxynivalenol. J Exp Bot *63*, 4731-4740.

Starkey, D.E., Ward, T.J., Aoki, T., Gale, L.R., Kistler, H.C., Geiser, D.M., Suga, H., Toth, B., Varga, J., and O'Donnell, K. (2007). Global molecular surveillance reveals novel Fusarium head blight species and trichothecene toxin diversity. Fungal Genet Biol *44*, 1191-1204.

Steffenson, B.J. (2003). Fusarium head blight of barley: Impact, epidemics, management, and strategies for identifying and utilizing genetic resistance. In Fusarium head blight of wheat and barley, K.J. Leonard, and W.R. Bushnell, eds. (St. Paul, MN, USA, American Phytopathological Society Press), pp. 241-295.

Talame, V., Bovina, R., Sanguineti, M.C., Tuberosa, R., Lundqvist, U., and Salvi, S. (2008a). TILLMore, a resource for the discovery of chemically induced mutants in barley. Plant Biotechnology Journal *6*, 477-485.

Talame, V., Bovina, R., Sanguineti, M.C., Tuberosa, R., Lundqvist, U., and Salvi, S. (2008b). TILLMore, a resource for the discovery of chemically induced mutants in barley. Plant Biotechnol J *6*, 477-485.

Varga, E., Wiesenberger, G., Hametner, C., Ward, T.J., Dong, Y.H., Schofbeck, D., McCormick, S., Broz, K., Stuckler, R., Schuhmacher, R., *et al.* (2015). New tricks of an old enemy: isolates of Fusarium graminearum produce a type A trichothecene mycotoxin. Environ Microbiol *17*, 2588-2600.
Vogt, T., and Jones, P. (2000). Glycosyltransferases in plant natural product synthesis: characterization of a supergene family. Trends in Plant Science *5*, 380-386.
Wang, H., Sun, S., Ge, W., Zhao, L., Hou, B., Wang, K., Lyu, Z., Chen, L., Xu, S., Guo, J., *et al.* (2020). Horizontal gene transfer of Fhb7 from fungus underlies Fusarium head blight resistance in wheat. Science *368*.
Waterhouse, A., Bertoni, M., Bienert, S., Studer, G., Tauriello, G., Gumienny, R., Heer, F.T., de Beer, T.A.P., Rempfer, C., Bordoli, L., *et al.* (2018). SWISS-MODEL: homology modelling of protein structures and complexes. Nucleic Acids Research *46*, W296-W303.
Wetterhorn, K.M., Gabardi, K., Michlmayr, H., Malachova, A., Busman, M., McCormick, S.P., Berthiller, F., Adam, G., and Rayment, I. (2017). Determinants and Expansion of Specificity in a Trichothecene UDP-Glucosyltransferase from Oryza sativa. Biochemistry *56*, 6585-6596.
Wetterhorn, K.M., Newmister, S.A., Caniza, R.K., Busman, M., McCormick, S.P., Berthiller, F., Adam, G., and Rayment, I. (2016). Crystal Structure of Os79 (Os04g0206600) from Oryza sativa: A UDP-glucosyltransferase Involved in the Detoxification of Deoxynivalenol. Biochemistry *55*, 6175-6186.
Xu, X.M., and Nicholson, P. (2009). Community Ecology of Fungal Pathogens Causing Wheat Head Blight. Annual Review of Phytopathology *47*, 83-103.
Zhu, H., Gilchrist, L., Hayes, P., Kleinhofs, A., Kudrna, D., Liu, Z., Prom, L., Steffenson, B., Toojinda, T., and Vivar, H. (1999). Does function follow form? Principal QTLs for Fusarium head blight (FHB) resistance are coincident with QTLs for inflorescence traits and plant height in a doubled-haploid population of barley. Theor Appl Genet *99*, 1221-1232.

FIGURE LEGENDS:

Figure 1: UGT13248 can alleviate DON induced root growth inhibition in barley seedlings.

A) – D) Two- to three-day old barley seedlings were transferred onto 0.5 x MS medium containing 1 mg / L DON (DON) or equal volumes of 70 % ethanol (mock). Root length was measured one day later (day1) and daily thereafter for 5 additional days. Data are from two to four independent experiments with 4-6 seedlings each combined. Means and SEM are shown. Asterisks indicated significant differences at $p < 0.01$ using Student's T-test comparing mock and DON samples for each time point within each genotype. A) and B) show results for two independent transgenic lines that express UGT13248 under control of *Zea mays* Ubi-1 promoter (UGT+), non-transgenic sister lines (UGT-), wild-type Golden Promise and Rasmusson. C) and D) show plants with mutations in UGT13248 T368I, H369Y and S403N as well as wild-type Morex seedlings.

Figure 2: **Protein models of UGT13248.**

Protein models based on the rice Os79 crystal structure are shown. Trichothecene is shown in purple, the non-reactive substrate UDP-2-fluoro-2-deoxy-D-glucose in orange, the conserved Thr299 and His38 residues in yellow and His369 and Thr368 in green. For T368I Thr at position 368 was replaced with Ile, for H369Y His at position 369 was replaced by Tyr and for S403N Ser at position 403 was replaced by Asn. Mutated residues are shown in pink.

Figure 3: UGT13248 catalyzes DON to D3G conversion in barley spikes.

A) Barley spikes of two sister lines one containing a *ZmUBi-1::UGT13248* transgene (UGT+) and one without (UGT-), were inoculated with 2 µg DON into 8 spikelets per spike at anthesis. Samples from two separate spikes were collected at the indicated time point and combined for each biological replicate. DON and D3G were measured. Data are shown as the mean ratio of D3G to DON of 3 independent biological replicates each and SEM. Asterisks indicate significant differences between UGT- and UGT+ at each time point at $p < 0.01$ using Student's T-test. B) Samples were treated and collected as described in A) for the indicated genotypes.

Figure 4: Mutations that reduce UGT13248 function result in increased susceptibility to *Fusarium graminearum* in the field. A) and B) Plants of the indicated genotypes were grown in the field, inoculated with *F. graminearum* at anthesis and scored 14 days later. For Morex, T368I, H369Y and S403N six independent rows and for Chevron and Stander three rows each per year (2019 or 2020) and environment (Saint Paul (SP) or Crookston (CR)) were used. For each biological replicate 10 spikes per row were evaluated for FHB severity and combined. Mean and SEM for three to six biological replicates each are shown. Asterisks indicate statistically significant differences from wild-type Morex at $p < 0.05$ using Student's T-test. C) to D) Three spikes per row for each year were collected in Saint Paul at the indicated time points and combined. DON and D3G were measured for four biological replicates each. Mean and SEM for D3G to DON ratio are shown. Asterisks indicate significant differences to wild-type Morex at each time point at $p < 0.01$ using Student's T-test.

Figure 5: UGT13248 is required for type II resistance. A) and C) photographs show representative images of spikes for each indicated genotype 14 (A) or 21 (C) days after point inoculation with *F. graminearum* PH-1. Scale bars are 1 cm. B) and D) Plants of the indicated genotypes were point inoculated in one central spikelet in the middle of the spike on each side the spike at anthesis. FHB severity was assessed at the indicated time points. 16-24 spikes each were assessed in two independent experiments and data were combined. Mean and SEM are plotted. Asterisks indicate statistically significant differences at $p < 0.05$ using Student's T-test.

Figure 6: *F. graminearum* spread and DON accumulation in the rachis was increased in H369Y compared to wild-type Morex plants. A)-C) Inoculated spikes at 14 days after inoculation with *F. graminearum* PH-1 were separated into five equal portions and rachis and spikelets were collected separately. The sections were labelled section 1 to section 5 from the basipetal portion of the spike to the most acropetal portion. Section 3 contained the inoculated spikelets. Samples from three spikes each were combined and four independent samples each were collected. A) Ergosterol as a proxy for fungal growth and B) DON was measured in each sample. Means and SEM are shown. Asterisks indicate significant differences between Morex and H369Y within each section and tissue at $p < 0.05$ using Student's T-test. C) Graphic depiction of date shown in A) and B). Colors indicate concentration of ergosterol and DON measured.

Figure 7: *F. graminearum* was observed within the rachis of T368I and H369Y but not wild-type Morex plants.

A) The junction between the most basipetal part of the spike and the peduncle of H369Y, T368I and wild-type sister lines (WT) for each allele, was imaged with confocal laser scanning microscopy 14 days after inoculation with *F. graminearum* (strain 8/1 (gpdAp::DsRed)). Scale bars are 200 µm. Blue color indicated autoflourescence, red color indicated fungal tissue. A 4x objective lens was used for both wild-type and mutant plants. A zoomed in image with a 10x objective lens was taken for both mutants. White squares indicate the region shown in higher

magnification at 10x. B) Rachis nodes of the indicated genotypes were imaged with confocal laser scanning microscopy 14 days after inoculation with *F. graminearum (*strain 8/1 (gpdA*p*::DsRed)). Rachis node at inoculated spikelet (inoculated) and four rachis nodes basipetal (basipetal) and four rachis nodes acropetal (acropetal) of the inoculated spikelet are shown. Scale bars are 200 µm. Blue color indicates autoflourescence, red color indicated fungal tissue.

1128 Table 1: Mutant and transgenic barley lines used in functional studies.

Line designation	**Type**	**Effect on *UGT13248***
Morex	TILLING background	none
T368I	TILLING mutant	nonsynonymous mutation
H369Y	TILLING mutant	nonsynonymous mutation
S403N	TILLING mutant	nonsynonymous mutation
Golden Promise	transformation background	none
#39003-UGT+	transformant	constitutive expression of *UGT13248*
#39009-UGT+	transformant	constitutive expression of *UGT13248*
#39003-UGT-	Non-transgenic sister line	none
#39009-UGT-	Non-transgenic sister line	none

1129

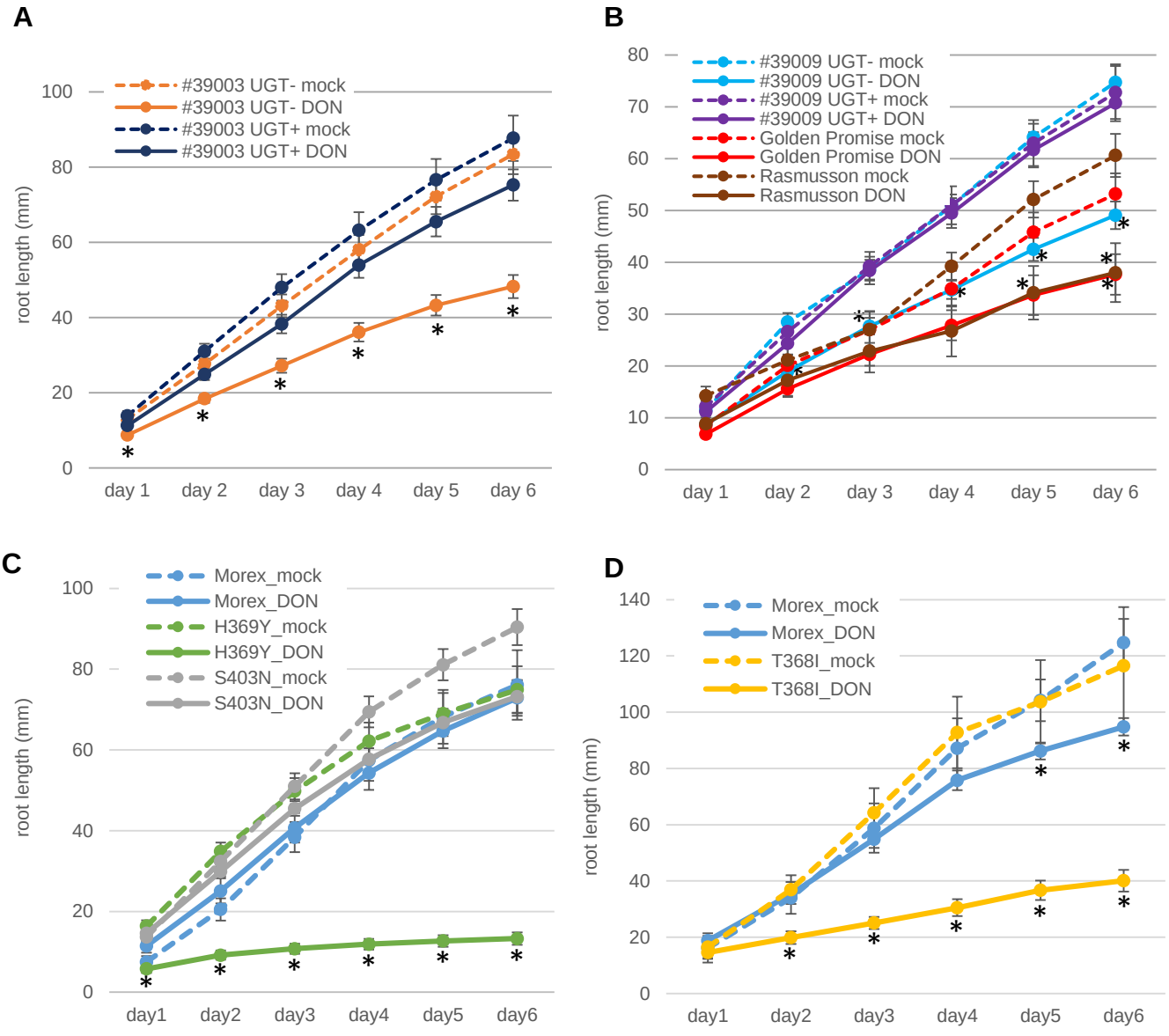

Figure 1: UGT13248 can alleviate DON induced root growth inhibition in barley seedlings.
A) – D) Two- to three-day old barley seedlings were transferred onto 0.5 x MS medium containing 1 mg / L DON (DON) or equal volumes of 70 % ethanol (mock). Root length was measured one day later (day1) and daily thereafter for 5 additional days. Data are from two to four independent experiments with 4-6 seedlings each combined. Means and SEM are shown. Asterisks indicated significant differences at $p < 0.01$ using Student's T-test comparing mock and DON samples for each time point within each genotype. A) and B) show results for two independent transgenic lines that express UGT13248 under control of *Zea mays* Ubi-1 promoter (UGT+), non-transgenic sister lines (UGT-), wild-type Golden Promise and Rasmusson. C) and D) show plants with mutations in UGT13248 T368I, H369Y and S403N as well as wild-type Morex seedlings.

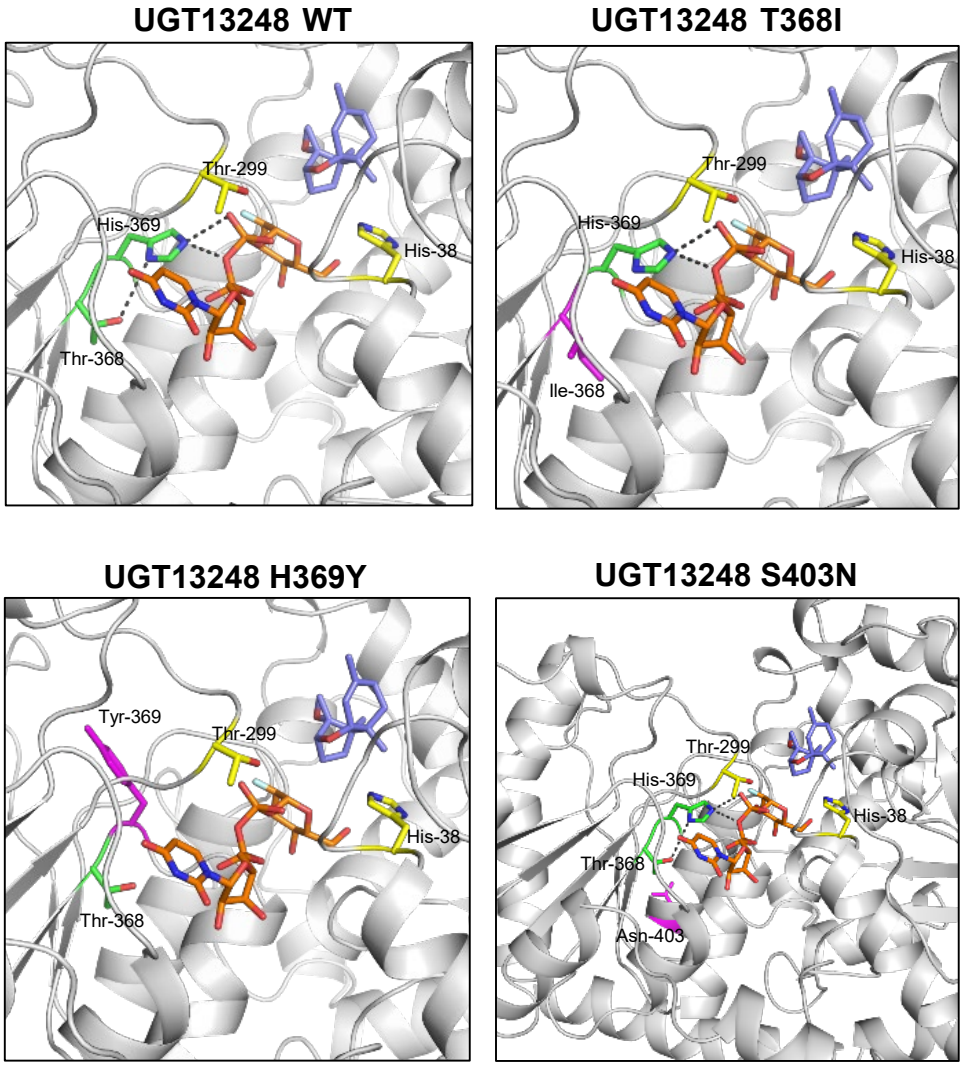

Figure 2: Protein models of UGT13248.
Protein models based on the rice Os79 crystal structure are shown. Trichothecene is shown in purple, the non-reactive substrate UDP-2-fluoro-2-deoxy-D-glucose in orange, the conserved Thr299 and His38 residues in yellow and His369 and Thr368 in green. For T368I Thr at position 368 was replaced with Ile, for H369Y His at position 369 was replaced by Tyr and for S403N Ser at position 403 was replaced by Asn. Mutated residues are shown in pink.

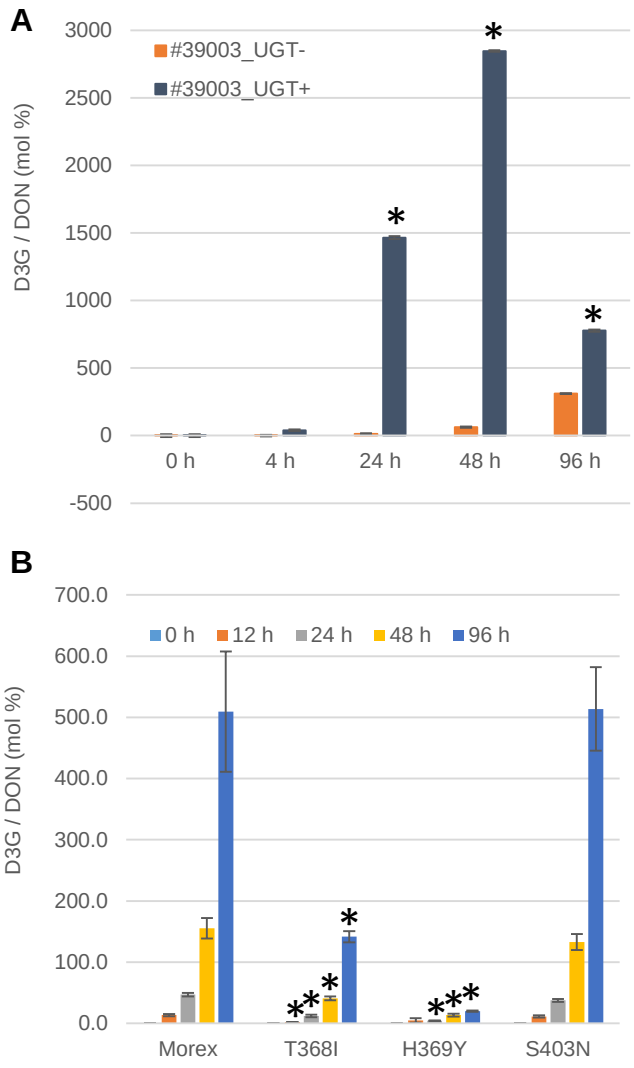

Figure 3: UGT13248 catalyzes DON to D3G conversion in barley spikes.
A) Barley spikes of two sister lines one containing a *ZmUBi-1::UGT13248* transgene (UGT+) and one without (UGT-), were inoculated with 2 µg DON into 8 spikelets per spike at anthesis. Samples from two separate spikes were collected at the indicated time point and combined for each biological replicate. DON and D3G were measured. Data are shown as the mean ratio of D3G to DON of 3 independent biological replicates each and SEM. Asterisks indicate significant differences between UGT- and UGT+ at each time point at $p < 0.01$ using Student's T-test. B) Samples were treated and collected as described in A) for the indicated genotypes.

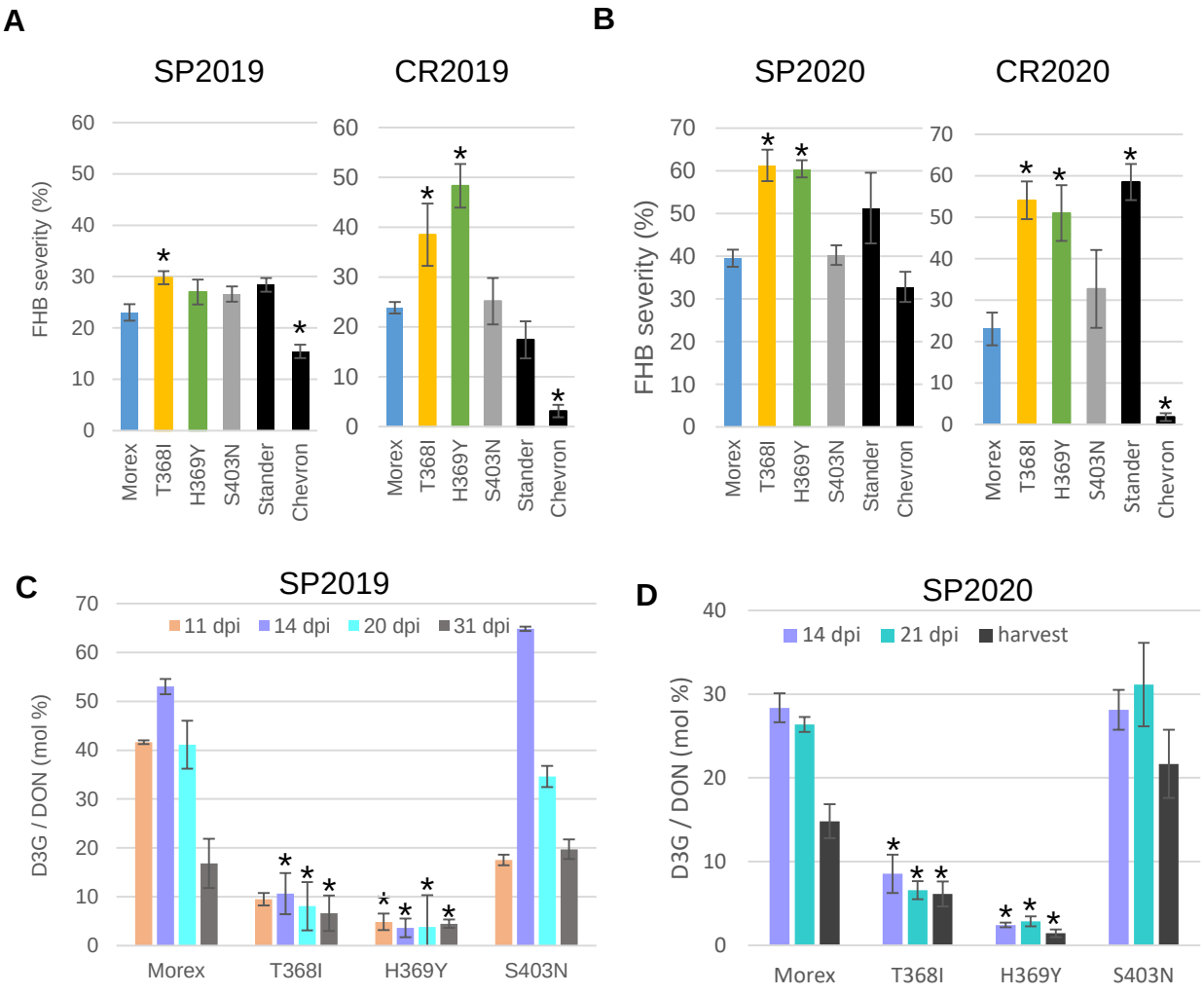

Figure 4: Mutations that reduce UGT13248 function result in increased susceptibility to *Fusarium graminearum* in the field. A) and B) Plants of the indicated genotypes were grown in the field, inoculated with *F. graminearum* at anthesis and scored 14 days later. For Morex, T368I, H369Y and S403N six independent rows and for Chevron and Stander three rows each per year (2019 or 2020) and environment (Saint Paul (SP) or Crookston (CR)) were used. For each biological replicate 10 spikes per row were evaluated for FHB severity and combined. Mean and SEM for three to six biological replicates each are shown. Asterisks indicate statistically significant differences from wild-type Morex at $p < 0.05$ using Student's T-test. C) to D) Three spikes per row for each year were collected in Saint Paul at the indicated time points and combined. DON and D3G were measured for four biological replicates each. Mean and SEM for D3G to DON ratio are shown. Asterisks indicate significant differences to wild-type Morex at each time point at $p < 0.01$ using Student's T-test.

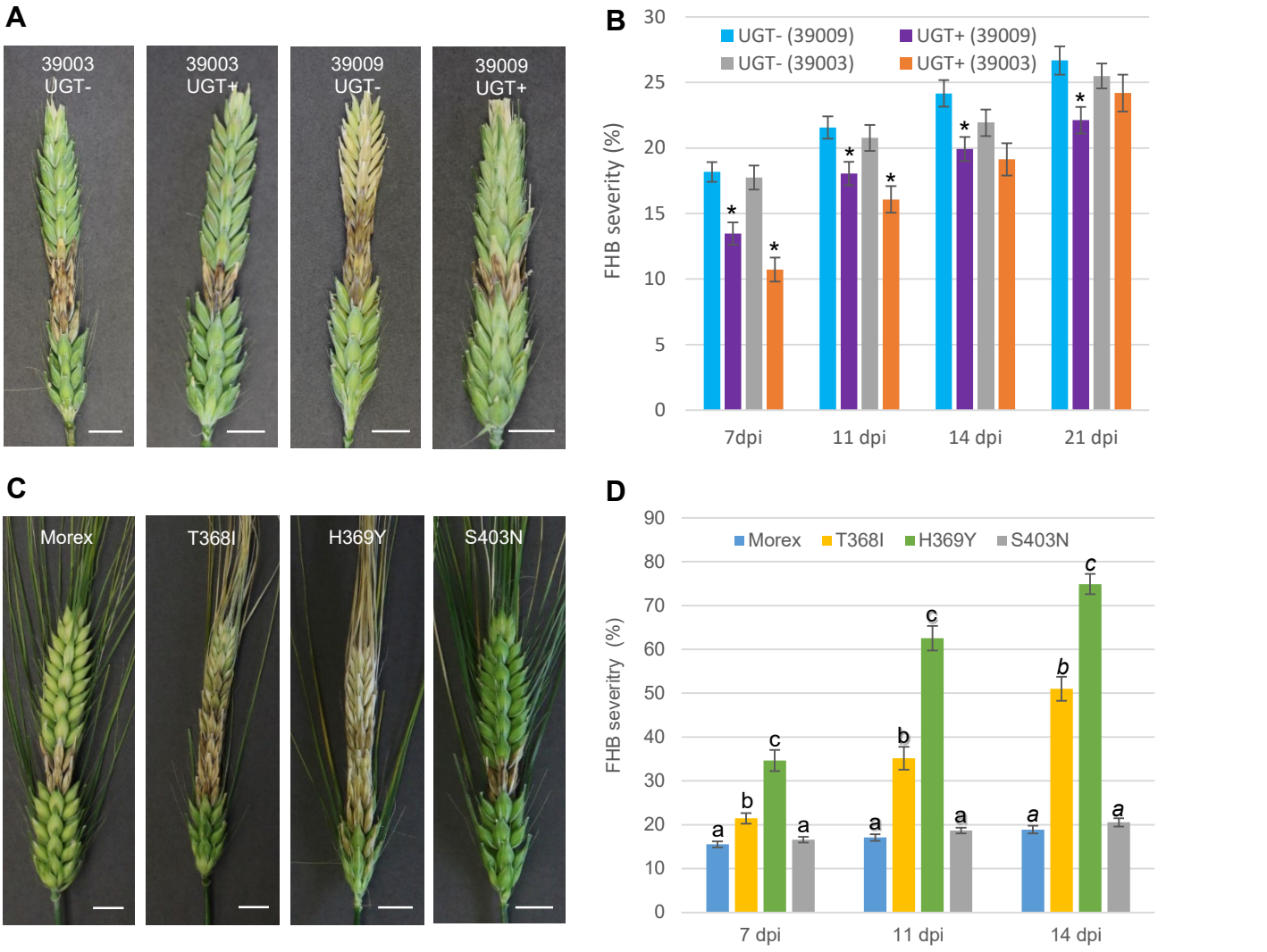

Figure 5: UGT13248 is required for type II resistance. A) and C) photographs show representative images of spikes for each indicated genotype 14 (A) or 21 (C) days after point inoculation with *F. graminearum* PH-1. Scale bars are 1 cm. B) and D) Plants of the indicated genotypes were point inoculated in one central spikelet in the middle of the spike on each side the spike at anthesis. FHB severity was assessed at the indicated time points. 16-24 spikes each were assessed in two independent experiments and data were combined. Mean and SEM are plotted. Asterisks indicate statistically significant differences at $p < 0.05$ using Student's T-test.

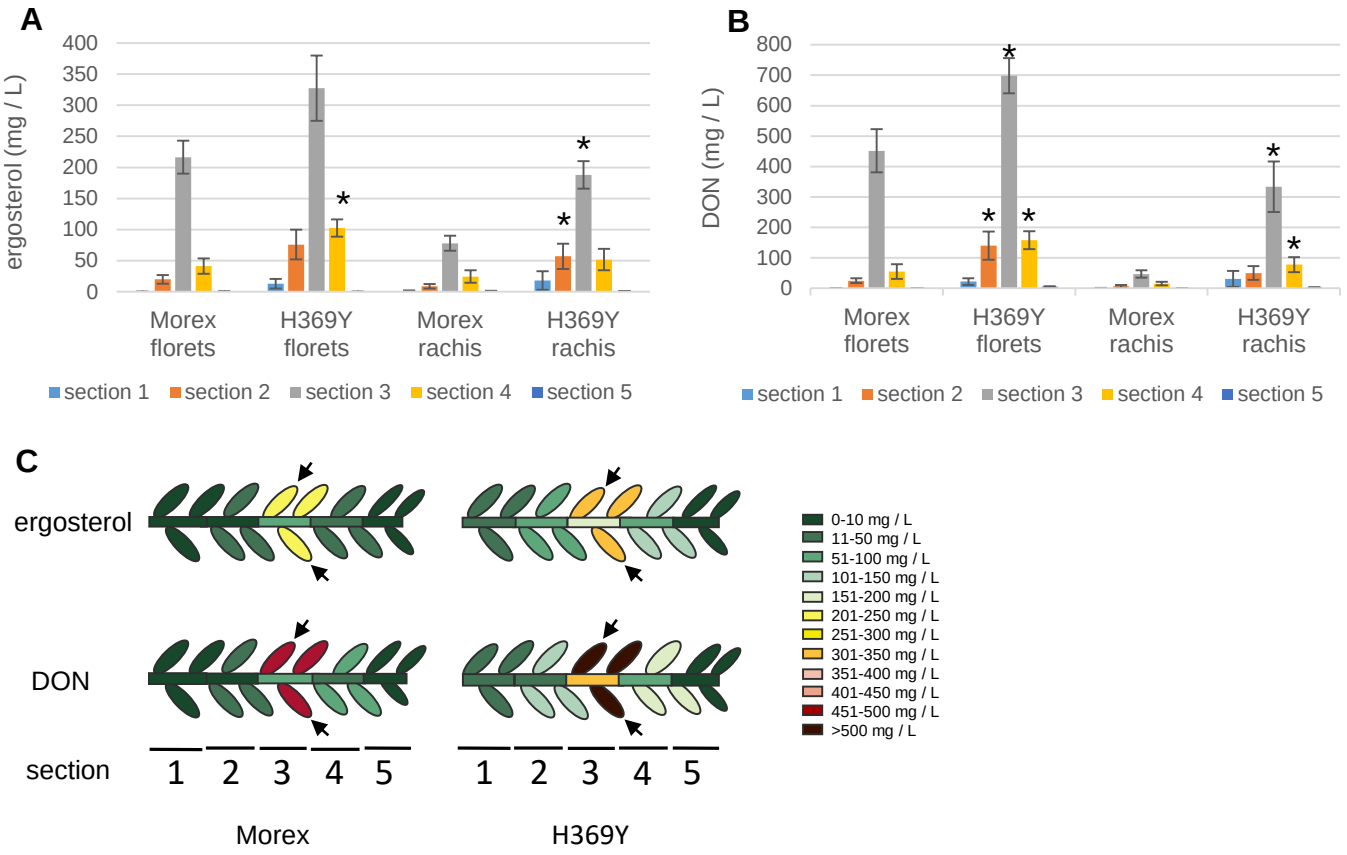

Figure 6: *F. graminearum* spread and DON accumulation in the rachis was increased in H369Y compared to wild-type Morex plants. A)-C) Inoculated spikes at 14 days after inoculation with *F. graminearum* PH-1 were separated into five equal portions and rachis and spikelets were collected separately. The sections were labelled section 1 to section 5 from the basipetal portion of the spike to the most acropetal portion. Section 3 contained the inoculated spikelets. Samples from three spikes each were combined and four independent samples each were collected. A) Ergosterol as a proxy for fungal growth and B) DON was measured in each sample. Means and SEM are shown. Asterisks indicate significant differences between Morex and H369Y within each section and tissue at $p < 0.05$ using Student's T-test. C) Graphic depiction of date shown in A) and B). Colors indicate concentration of ergosterol and DON measured.

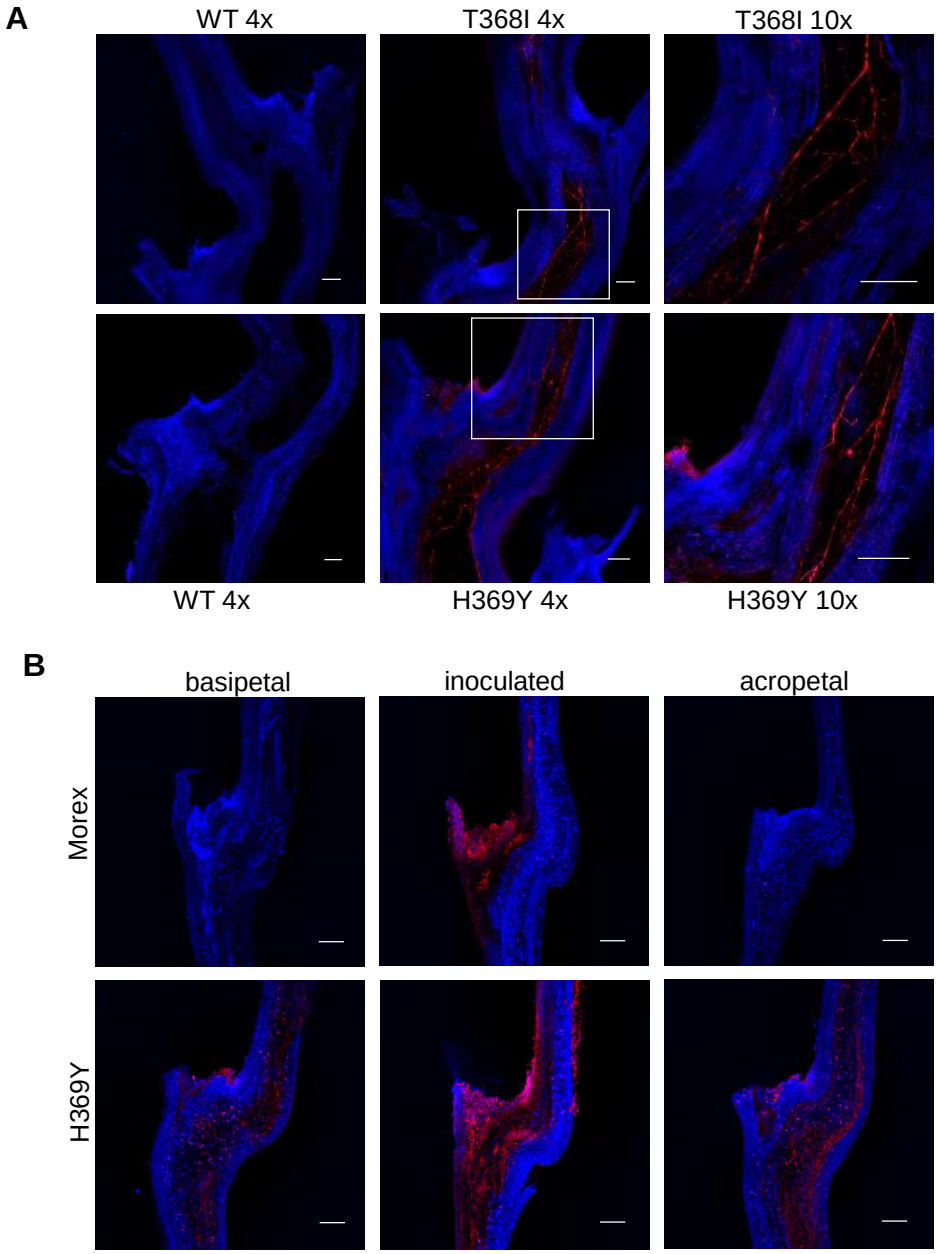

Figure 7: *F. graminearum* was observed within the rachis of T368I and H369Y but not wild-type Morex plants. A) The junction between the most basipetal part of the spike and the peduncle of H369Y, T368I and wild-type sister lines (WT) for each allele, was imaged with confocal laser scanning microscopy 14 days after inoculation with *F. graminearum* (strain 8/1 (gpdAp::DsRed)). Scale bars are 200 µm. Blue color indicated autoflourescence, red color indicated fungal tissue. A 4x objective lens was used for both wild-type and mutant plants. A zoomed in image with a 10x objective lens was taken for both mutants. White squares indicate the region shown in higher magnification at 10x. B) Rachis nodes of the indicated genotypes were imaged with confocal laser scanning microscopy 14 days after inoculation with *F. graminearum (*strain 8/1 (gpdA*p*::DsRed)) using a 4x objective lens. The rachis node at the inoculated spikelet (inoculated) and four rachis nodes basipetal (basipetal) and four rachis nodes acropetal (acropetal) of the inoculated spikelet are shown. Scale bars are 200 µm. Blue color indicated autoflourescence, red color indicated fungal tissue.